

### 3. SITE 337

The Shipboard Scientific Party<sup>1</sup>

With Additional Contributions From

Svein B. Manum, Universitetet i Oslo, Oslo, Norway

H. Raschka and F.-J. Eckhardt, Bundesanstalt für Geowissenschaften und Rohstoffe, Hannover, Germany and

H.-J. Schrader, Der Universität Kiel, Kiel, Germany

#### SITE DATA

**Position:** 64°52.30'N; 05°20.51'W

**Water Depth (from sea level):** 2631.0 corrected meters (echo sounding)

**Bottom Felt at:** 2657.0 meters (drill pipe)

**Penetration:** 132.5 meters

**Number of Holes:** 1

**Number of Cores:** 15

**Total Length of Cored Section:** 132.5 meters

**Total Core Recovered:** 98.5 meters

**Percentage of Core Recovery:** 74.3%

#### Oldest Sediment Cored:

Depth below sea floor: 113.0 meters

Nature: Dusky yellow clay

Age: Early or middle Oligocene (Core 12)

Measured velocity: 153 km/sec

#### Basement

Depth below sea floor: 113.0 meters (drilled)

Nature: Basalt

Age: K/Ar—18-24 m.y. (late Oligocene to early Miocene)

**Principal Results:** Site 337 is located on what are believed to be rift mountains just east of the "extinct" spreading axis in the Norway Basin. Drilling penetrated a total depth of 132.5 meters, of which 113 meters was in sediment, and the remainder in basalt. The sediment section includes about 47 meters of "glacial" sediments consisting of clays, sandy muds and muds, and glacially derived material such as pebbles. The Tertiary unit ranging to the lower/middle Oligocene(?) is an almost completely pelagic accumulation of clay and muds. Basement consists of basalt very similar to tholeiitic basalt typically found in mid-ocean ridge rifts. Brecciated layers suggest the presence of 13-14 flows of pillow lavas. Using the tentative age obtained for the oldest sediments and radiometric determinations and making a very rough allowance of distance from the axis of

"extinct" rift, it is estimated that the shift in ridge axis from the Norway Basin took place about 25 m.y. ago.

#### BACKGROUND AND OBJECTIVES

The primary objective of drilling at Site 337 was to learn about the age and history of the Norway Basin. Has it been formed by submergence of an epicontinental sea, or by sea-floor spreading? In particular, if it has been created by sea-floor spreading, what is the date at which spreading stopped here and the spreading axis shifted elsewhere?

The location and rough bathymetry of the Norway Basin are shown in Figure 1. The situation of the axis of spreading axis north of Iceland is peculiar, in that the axis of spreading along the Iceland-Jan Mayen Ridge is situated symmetrically between Norway and Greenland. There is no deep basin west of the Iceland-Jan Mayen Ridge. The only deep basin is the Norway Basin, which lies to the east, and is separated from the active Iceland-Jan Mayen Ridge by the apparently inactive Jan Mayen Ridge.

The asymmetric situation of the present spreading axis led to the suggestion by Johnson and Heezen (1967) that the axis of spreading has, after formation of the Norway Basin, shifted west of the Jan Mayen Ridge. If this were the case, an "extinct spreading axis" should exist in the Norway Basin and be associated with a set of bilaterally symmetrical magnetic anomalies.

Vogt et al. (1970) reported the existence of symmetrical magnetic anomalies in the Norway Basin. However, the identification of these anomalies is not certain. Vogt et al. (1970) believed that the date of the axial anomaly is 42 m.y., while LePichon et al. (1971), from the same data, believe that the date of cessation of spreading in the Norway Basin is 49 m.y., which is the date associated with the axial anomaly.

Talwani and Eldholm (in press) from a number of surveys in the Norway Basin have defined the position of a structural valley (Figure 1) which extends across the Norway Basin with roughly a northeast-southwest trend. Because of burial by sediments, the valley is less clearly defined bathymetrically in the north, but free-air gravity profiles clearly delineate it. The magnetic anomaly profiles show symmetry with respect to the valley in all cases, a magnetic maximum exists above the valley. For this reason Talwani and Eldholm (in press) believe that this valley also defines the "extinct axis of spreading" in the Norway Basin.

There is another point of interest in connection with the date of shift of the spreading axis from the

<sup>1</sup>Manik Talwani, Lamont-Doherty Geological Observatory, Palisades, New York; Gleb B. Udintsev, P.P. Shirshov Institute of Oceanology, Moscow, USSR; Kjell Bjørklund, Universitetet i Bergen, Bergen, Norway; V.N.D. Caston, British Petroleum Company Ltd., Middlesex, England; Richard W. Faas, Lafayette College, Easton, Pennsylvania; Jan E. van Hinte, Esso Production Research Company, Begles, France; G.N. Kharin, Atlantic Branch of Oceanology Institute, Kaliningrad, USSR; David A. Morris, Phillips Petroleum Company, Bartlesville, Oklahoma; Carla Müller, Geologisch-Paleontologisches Institut der Johann Wolfgang Goethe-Universität, Frankfurt am Main, Germany; Tor H. Nilsen, U.S. Geological Survey, Menlo Park, California; Detlef A. Warnke, California State University, Hayward, California; Stan M. White, University of California at San Diego, La Jolla, California.

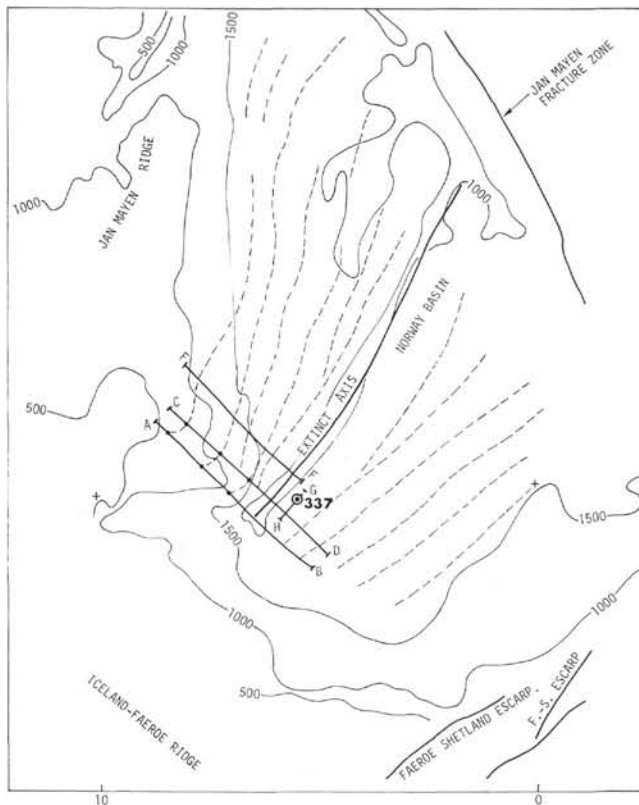


Figure 1. Location and bathymetry of the Norway Basin (contours in uncorrected fathoms).

Norwegian Sea. Three stages are generally accepted in the evolution of the portion of the Atlantic north of the Azores-Gibraltar Ridge, that is, the portion of the North Atlantic created by the drifting apart of North America from Europe. During the first stage which lasted up to about 60 m.y., the separation of Eurasia from North America took place in the Labrador Sea. During this stage, the Norwegian-Greenland Sea had not started to open, and Greenland was attached to Eurasia. During the second stage, which lasted from 60 m.y. to 40 m.y., the Labrador Sea continued to open, but a second opening also began between Greenland and Norway. Thus the Labrador Sea and the Norwegian Sea were opening simultaneously. At the end of this stage, the motion of Greenland with respect to North America stopped. The separation between Greenland and Norway continued, but along a more easterly azimuth. This change of direction of relative motion, which is reflected in a change of azimuth in the fracture zones, is an important event in the evolution of the Norwegian Sea. It is of interest to learn whether the shift of axis from the Norway Basin was coincident with the change in direction of spreading in the Norwegian Sea.

In selecting the exact site for location of the drill hole, it was desired to be as close to the axis of the valley as possible. However, the thickness of sediments in the valley is so large that it was not expected that basement would be reached there. A site survey was made near the southern part of the extinct axis, and on the basis of this survey, a site was selected which lies on

top of the "extinct rift mountains" east of the axis. The seismic reflection profile G-H (Figure 1), which was run parallel to the axis, shows a sediment thickness of about 400 meters (assuming a velocity of sound of 2 km/sec in sediments) at the site selected for drilling (Figure 2).

Note that as far as the magnetic anomaly is concerned, this site lies on the sharp gradient east of the axial maximum shown in profiles A-B and C-D (Figures 1, 3).

### Summary of Objectives at Site 337

1. To obtain a date for basement at the "extinct spreading axis" in the Norway Basin.
2. Examine the sedimentary history in the Norway Basin. In particular, look for the hiatus between the Pleistocene and the Oligocene observed at Site 336 (on the Iceland-Faeroe Ridge).
3. Faunal and climatic study objectives are roughly similar to those for Site 336.

## OPERATIONS

### Approach to Site 337

Site 337 was approached from the southwest at a heading of 053° (at 0500Z) after steaming some 86.5 nmi from Site 336. At 0702Z, the speed was reduced to 170 rpm, and at 0708Z, the heading was changed to 046°. At 0935Z, the heading was changed to 045°, and 16-kHz ORE beacon was dropped at 1046 on 10 August. After testing the beacon, *Glomar Challenger* maneuvered and locked on target (Figure 4).

### Drilling Operations

On completion of core line respooling, the same BHA and bit type as employed at Site 336 was run. After flushing out the drill stem, the core barrel was inserted, and sea bed was touched at 2657 meters (drill string measurement).

Continuous coring commenced at 0130 hr, 11 August, and continued to a total depth of 2789.5 meters. The sediments were cored with generally good recovery (86 m recovered from 113.5 m cored—75.6%) (Table 1). Poor recoveries from Cores 6 and 8 are attributed to very soft clay material. Fortunately, the lower 0.5 meters of recovery from Core 12 included the contact to basalt. Particular care was taken in cutting and obtaining this core, because "soft" type core catchers were being used. From the 19 meters of basalt cored, 12.5 meters (66%) was recovered. Overall recovery was 98.5 meters from 132.5 meters cored, or 74% (Table 1).

No evidence of hydrocarbon was encountered, although there was some gaseous expansion from some cores possibly due to CO<sub>2</sub>. The hole was abandoned according to the relevant safety regulations, and the BHA retrieved above the sea bed by 0320 hr, 12 August. *Glomar Challenger* was underway for Site 338 at 0835 hr.

## LITHOLOGY

Sediments and rocks from Hole 337 included 86 meters of unconsolidated sediments, overlying 12.5 meters of basalt. Two sediment units (Units 1 and 2) and one basalt unit (Unit 3) were differentiated (Figure

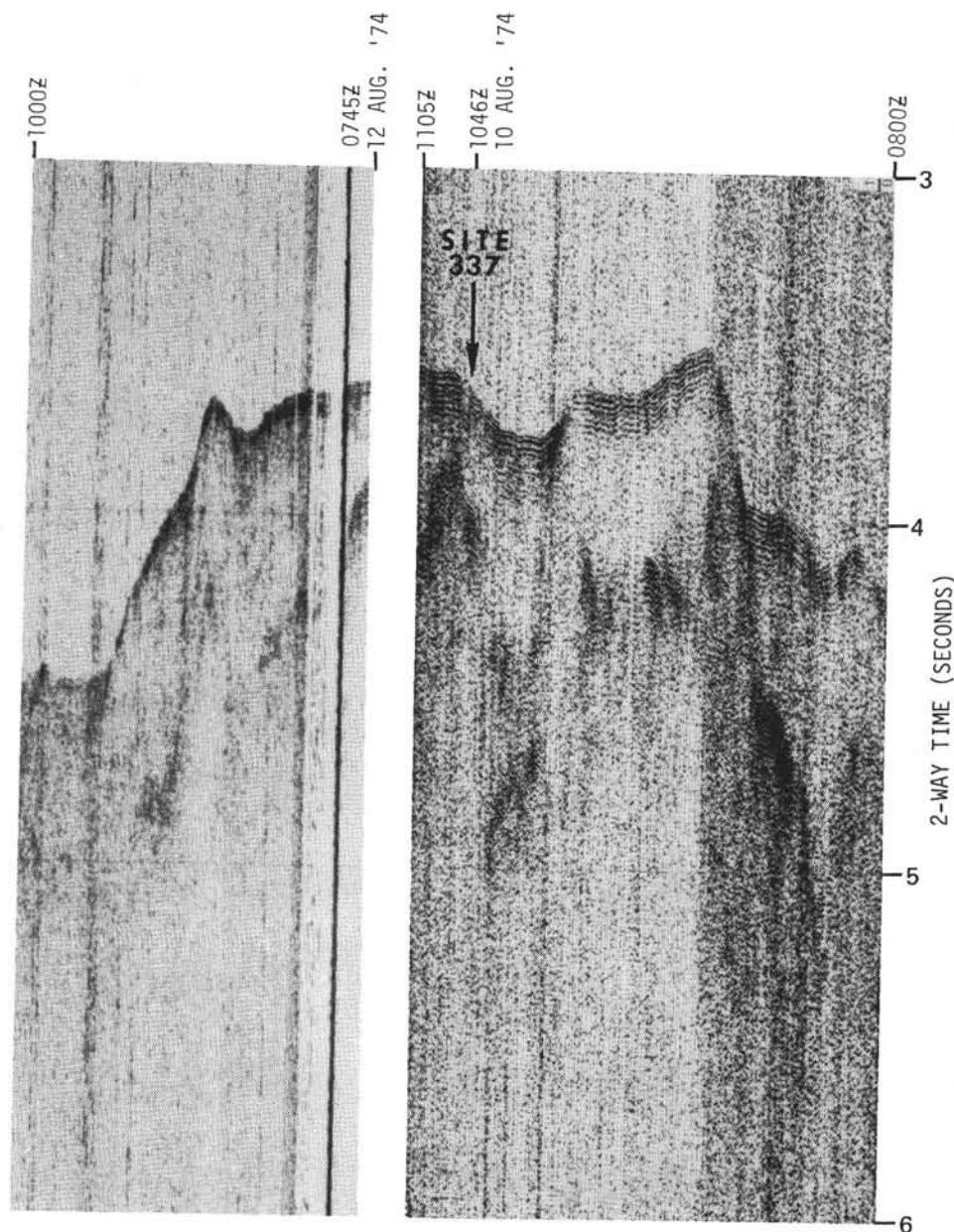


Figure 2. Profiler record, Site 337.

5). Unit descriptions and significant characteristics are found in Table 2.

### Unit Descriptions

#### Unit 1

Unit 1 consists of a 47-meter-thick-series of predominant muds, with intercalated ash and calcareous biogenic oozes. Two subunits have been defined: Subunit A (0-18.5 m), which generally has yellow-brown to pale dusky brown colors; and Subunit B (18.5-47 m) with olive and/or gray colors. The color change between subunits is gradational.

The sediments of Subunit A have been intensely disturbed by coring/drilling, however, the color diversity in any one section or core seems to imply the presence of pre-existing stratification (0.5-3 cm thick). The sediments consist primarily of muds, with interbedded

nannofossil oozes and ash streaks. Also common are clay or sandy mudstone pebbles (up to 15 mm), clay or claystone balls or clasts, and sand-sized *Globorotalia*. In Core 2, greenish-gray and olive-gray colors are present and appear to grade into the gray colors of Subunit B.

Subunit B is similar to Subunit A, with some noticeable differences. In Subunit B, interbedded nannofossil oozes are more prevalent (Table 2) and clay clasts are scattered throughout. The subunit becomes more consolidated starting in Core 4, Section 3 and in Core 5, Section 2, allowing stratification to be easily identified. Bedding thicknesses range from 2 to 30 mm (average 5 mm). They are distinguished primarily by color, but also represent different lithologies (clay versus mud). The clay tends to be most competent.

All grain size analyses show mud as the dominant textural classification. The sand content ranges from 0.2% to 24%, and, in general, the content is lowest near

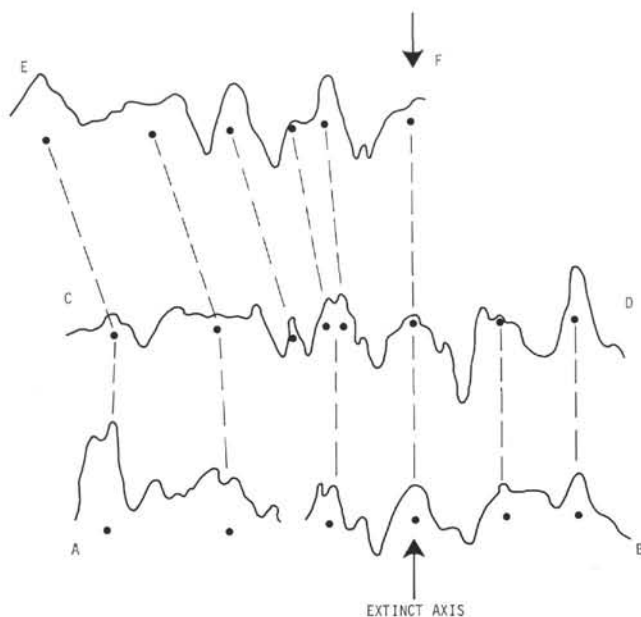


Figure 3. Profile Sections E-F, C-D, and A-B, of Figure 1.

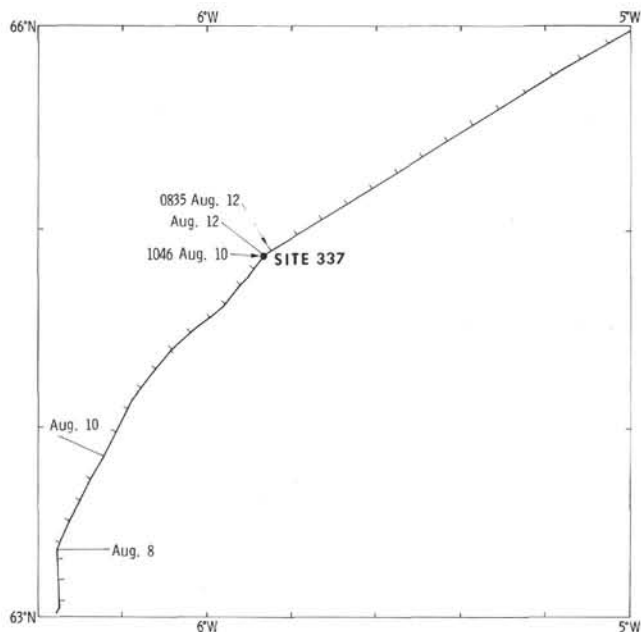


Figure 4. Track chart, Site 337.

the base of the unit.  $\text{CaCO}_3$  percentages are variable from 1% to 54%, the higher values representing nanofossil ooze zones.

#### Unit 2

Unit 2 is a thick (70.8 m) sequence of mud with some clay, and with yellow, orange, and brown colors (Table 2). It is separated from Unit 1 by a sharp contact at 42.2 meters (Core 5, Section 4) and is characterized by clay balls and/or clasts, small (5-15 mm) Mn(?) zones (pebbles, patches, or concretions?), zeolite patches, sub-horizontal and indistinct stratification, and volcanic ash zones and strata. Zeolites are a significant (5%-25%) component in Cores 6 and 7.

Carbon dioxide was present in measurable amounts in Core 7, Section 2 to Core 7, Section 4, and its presence completely homogenized the cores. On visual inspection, the gas appeared to continue in lesser quantities through Core 10. It is suggested that it is a result of local diagenetic reactions within the sediment column.

Four grain size analyses indicate mud as the dominant sediment, with the sand content less than 4%. Five  $\text{CaCO}_3$  samples contain 0%-1%  $\text{CaCO}_3$ , reflecting the absence of calcareous nanofossils in Unit 2.

#### Interpretations

The sedimentary sequence at Site 337 has components derived from terrigenous, volcanic, and biogenic sources. For the most part, the sediments represent pelagic accumulations, with additional contributions from ice rafting.

1) Unit 2 (Core 5, Section 4 to Core 12, Section 5) overlies the basalt and appears to represent a thick accumulation of pelagic clay below the CCD, during the lower (?) Oligocene. Calcareous fossils are nonexistent, while siliceous fossils (radiolarians, diatoms, sponge spicules) are present in limited amounts, but increasing below Core 9. Volcanic ash zones (or strata), zeolite clay zones indicate a substantial volcanic contribution to the Norway Basin sediments during this time. For the most part, the zeolite (phillipsite?) represents in situ alteration of volcanic materials.

Some indistinct bedding is observed (Cores 7, 10, 11, and 12) in the dominant yellow mud and clay, as well as volcanic ash laminae. Mn micronodules and trace amounts of glauconite, indicate a reasonably low sedimentation rate.

2) Subunit B, the lowest subunit of Unit 1 (Table 2), represents deposition of sediments derived from terrigenous sources. Stratification is first noticeable in Core 5, Section 2, and improves to the base of the subunit (Core 5, Section 4). Clay balls or clasts are common, and a size grading is indicated by the distribution of the mud, clay, and sandy mud interbeds. Local zones of lithification (claystone, mudstone) are also present in Core 5.

3) The deposition of Subunit A was probably gradational from Subunit B, seemingly indicating a similar depositional process. The presence of pebbles (sandy mudstone, chert, limestone, and basalt) points to ice rafting as a significant sediment contributor. Volcanic ash is present, but the relative amounts seem less compared to Unit 2, considering the different rates of sedimentation. As in Subunit B, the presence of nanofossil oozes and foraminifera indicates deposition above the CCD.

#### IGNEOUS PETROGRAPHY-PETROLOGY-GEOCHEMISTRY

##### General

Basalt was recovered from Cores 12, CC, 13, 14, and 15. Based on a megascopic examination, the basement rock consists of altered and brecciated aphyric, sparsely aphyric, amygdaloidal basalts, and basalt breccia. Aphyric basalt is predominant, being dark gray to dark black, with rare olivine phenocrysts. The amygdaloidal

TABLE 1  
Coring Summary, Site 337

Core	Date (August 1974)	Time	Depth From Drill Floor (m)	Depth Below Sea Floor (m)	Cored (m)	Recovered (m)	Recovery (%)
1	11	0245	2657.0-2666.0	0-9.0	9.0	8.5	94
2	11	0345	2666.0-2675.5	9.0-18.5	9.5	9.5	100
3	11	0500	2675.5-2685.0	18.5-28.0	9.5	9.5	100
4	11	0630	2685.0-2694.5	28.0-37.5	9.5	6.2	65
5	11	0725	2694.5-2704.0	37.5-47.0	9.5	7.5	79
6	11	0845	2704.0-2713.5	47.0-56.5	9.5	2.7	28
7	11	0945	2713.5-2723.0	56.5-66.0	9.5	9.5	100
8	11	1045	2723.0-2732.5	66.0-75.5	9.5	2.2	23
9	11	1150	2732.5-2742.0	75.5-85.0	9.5	7.9	83
10	11	1257	2742.0-2751.5	85.0-94.5	9.5	9.4	99
11	11	1350	2751.5-2761.0	94.5-104.0	9.5	7.7	81
12	11	1520	2761.0-2770.5	104.0-113.5	9.5	5.4	57
13	11	1850	2770.5-2780.0	113.5-123.0	9.5	5.5	58
14	11	2250	2780.0-2785.5	123.0-128.5	5.5	4.5	82
15	12	0210	2785.5-2789.5	128.5-132.5	4.0	2.5	62
Total			2789.5	132.5	132.5	98.5	74

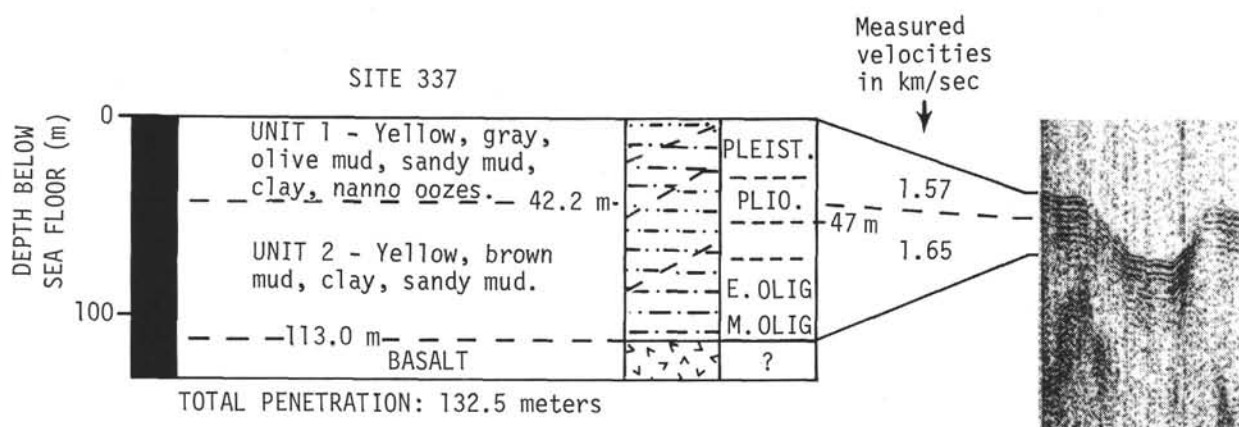


Figure 5. Lithologic column and seismic profile, Site 337.

basalt is gray, containing nearly 10% or more amygdules filled with chlorite, smectite, and calcite. The basaltic breccia consists of fragments of aphyric, amygdaloidal, phyrlic basalts, basaltic glass, palagonite, and chlorite, in a calcite-chlorite-smectite matrix.

There are 14 breccia horizons which are probably surfaces of a pillow lava, which has been very highly altered. The entire section is broken by fissures and slickensides. There are numerous calcite, chlorite, and smectite veins.

### Petrography

Microscopic studies provide additional evidence of importance on the basement rocks, aphyric and microporphyrlic basalts, and hyalobasalts with rare phenocrysts. Of lesser importance, are sparsely phyrlic variolitic basalts, amygdaloidal basalts, and basaltic breccia.

#### Variolitic Basalt

The texture is variolitic, microporphyrlic, and is characterized by an irregular crystallization. Most crystalline areas (varioles) have a leucocratic composition, have a spotty arrangement, and indistinct bound-

aries. Varioles consist of thin skeletal plagioclase laths growing from a single center and having split ends. Often varioles represent tufts of unordered plagioclase laths. Radiating-fibrous tufts of clinopyroxene are also arranged in gaps among the varioles. They are generally decomposed and replaced by microfoliated aggregates of hydrobiotite. The hydrobiotite is decomposed with the development of varying quantities of hydrogoethite. Separate gaps contain fine fibrous magnetite, also arranged in a radiating pattern. Phenocrysts of olivine and clinopyroxene (0.1-1.0 mm) contained in varioles, are generally arranged glomeroblastically. The grains are idiomorphic-like, separate phenocrysts are underdeveloped.

Olivine is highly altered and replaced by reddish-brown iddingsite, which is arranged in joints. Plate-like iddingsite covers the grain surface in mutually perpendicular directions. The quantity of olivine often reaches 10% and more (Sample 15-2, 9-12 cm), thus one can define an olivine variolitic basalt. Melted plagioclase phenocrysts are rare. Large separate laths of plagioclase (up to 1.5 mm) are intergrown in the groundmass, which is mainly leucocratic and consists of radiating tufts of fine-grained clinopyroxene with

TABLE 2  
Lithologic Summary, Site 337

Unit	Depth (m) and Core Numbers <sup>a</sup>	Age	Characteristics
1	0.0-18.5 (1)-(2)		Color mottling due to intense deformation in upper cores, large forams ( <i>Globorotalia</i> ), pebbles (sandy mudstone, basalt (weathered), chert, black limestone, clay clasts);
Subunit A		Pliocene and Pleistocene	Interbedded nanofossil oozes (1-2), (1-4), (1-5), (2-5), (3, CC), ash streaks (1-2) (1-6), terrigenous mineral components.
	18.5-47.0 (3)-(5, CC)		Clay balls or clasts common, ash streaks at (3-2), (4-2); interbedded nanofossil oozes (3-5), (4-1), (4-3), (4-4), (5-1), (4, CC), (5-3); local lithification (5-2); stratification first noticeable in (5-2), good in 5-3; terrigenous mineral components
Subunit B			
2	47.0-113.0 (6)-(12-5)	Undated 47.0-75.5 m, the remainder is early or middle Oligocene	Indistinct laminations, claystone fragments, mottling; zeolitic clay zones in Section 6-2; disseminated Mn (nodules) mudstone, and volc. ash clasts present to Cores 10, 11; ash (6-2), (7-4), (8-2), (7-3), (9-4), (10-6); CO <sub>2</sub> gas in Core 7; clay mud (zeolitic in Cores 6, 7-CC, 11-5); terrigenous mineral components. No calcareous fossils, but siliceous are present and increase in numbers downward
3	113.0-132.5 (12-5)-(15)	?	Basalt with extensive calcite or chlorite-filled veins, brecciated zones, and highly vesicular nature

<sup>a</sup>Core numbers in parentheses.

spotted interference colors. Rare oval and round pores are filled by smectite and hydrogoethite (see Kharin, this volume).

#### Variolitic Hyalobasalt

The basalt has a variolitic structure of its groundmass in combination with a hyaline structure. Glassy groundmass occupies 25%-30% of the thin section surface. A large number of amygdules (up to 10%-12%), formed by smectite and calcite, are present (see Kharin, this volume).

#### Amygdaloidal Variolitic Basalt

It is distinguished from the variolitic basalt based on the presence of a large number (10%-20%) of round

amygdules, formed of smectite, calcite, zeolite, and a mixture of these minerals (see Kharin, this volume).

#### Aphyric Variolitic Basalt

The structure and texture are analogous to variolitic basalts, but differ from them by the lesser amount or absence of phenocrysts. Rare inclusions of olivine are replaced by iddingsite and goethite. There are rare amygdules of calcite and smectite and fine veins of smectite.

#### Basaltic Breccia

Fragments of variolitic basalt consist of plagioclase laths (30%), and branched clinopyroxene (60%-70%). There are also rare olivine phenocryst relics (0.3-0.8 mm), replaced by iddingsite, chlorophite, chlorite, and calcite. Small skeletal plagioclase phenocrysts are very rare. Very small angular fragments of magnetite (1%-2%) are evenly distributed over the thin section area. Fragments of basalt are cemented by calcite plus chlorite and smectite. The cement contains angular fragments of chlorite, which was probably formed as result of replacement of fragments of volcanic glass.

#### Discussion

Volcanic rocks of acoustic basement at Site 337 are represented by poorly crystallized basaltic lavas which flowed and cooled quickly in submarine conditions. The presence of brecciated horizons with altered volcanic glass leads us to suggest that the hole penetrated through 13-14 flows of pillow lavas, separated by surfaces of volcanic glass. The presence of amygdaloidal basalts originating from porous pillow lavas also supports this conclusion. The basalts of Site 337 are very similar to oceanic olivine tholeiitic basalts typical of mid-ocean ridges and oceanic plates (seamounts). However, they are intensively altered, brecciated, chloritized, calcified, and contain extensive goethite.

#### Geochemistry (H.J. and F.-J.E.)

Chemical analyses and norms for the Site 337 basalts are shown in Table 3. Although the petrographic description mentions 13 to 14 pillow flows, the major element chemistry of samples of the different cores is rather uniform. Fresh basalts are absent: H<sub>2</sub>O<sub>total</sub> = 2.35%-3.77%; 100 FeO/FeO + Fe<sub>2</sub>O<sub>3</sub> = 39.9-68.4.

The average major element concentrations are similar to ocean floor basalt (Cann, 1971): Al<sub>2</sub>O<sub>3</sub> with an average of 15%, a little to high K<sub>2</sub>O content (0.33% average). Only TiO<sub>2</sub>, with an average of 1.05%, is lower than the Site 336 basalts of ocean floor character.

Some trace elements are even more depleted than at Site 336 (Table 4):

average Sr:	72 ppm
Zr:	53 ppm
Rb:	around 5 ppm.

Ni and Cr contents are slightly enriched corresponding to Mg. Within Yoder and Tilley's (1962) division of basalts, the rocks may be classed mainly as olivine-tholeiite, and subordinately as quartz-normative tholeiites. The crystallization index (total Fe as FeO/MgO) of 1.30 approaches the low values of the

TABLE 3  
Analyses of Site 337 Basalts

	13-1, 135-138 cm RF 9788	13-2, 37-40 cm RF 9789	13-2, 140-143 cm RF 9790	13-3, 38-41 cm RF 9791	14-1, 142-145 cm RF 9793	14-1, 74-77 cm RF 9794	14-2, 91-94 cm RF 9795	14-3, 6-11 cm RF 9796	14-3, 128-131 cm RF 9797	15-1, 127-130 cm RF 9798	15-2, 9-12 cm RF 9799	15-2, 41-44 cm RF 9800	15-2, 97-100 cm RF 9801	15-2, 137-140 cm RF 9802
SiO <sub>2</sub>	47.03	48.14	48.06	48.48	48.01	48.96	48.72	47.71	47.45	47.27	47.65	46.65	46.92	48.06
TiO <sub>2</sub>	1.01	1.03	1.09	1.11	1.06	1.05	1.05	1.10	1.04	1.02	1.02	0.99	1.01	1.07
Al <sub>2</sub> O <sub>3</sub>	14.41	14.74	15.61	15.99	15.13	15.17	15.21	15.74	14.85	14.65	14.66	14.32	14.39	15.30
Fe <sub>2</sub> O <sub>3</sub>	6.89	3.28	4.72	3.91	5.59	3.69	3.98	4.63	5.20	4.10	6.44	4.76	6.08	4.25
FeO	4.53	7.09	5.30	5.13	5.55	6.33	6.08	5.36	5.06	5.99	5.34	5.44	5.28	5.50
MnO	0.15	0.17	0.13	0.15	0.16	0.18	0.17	0.16	0.15	0.17	0.16	0.17	0.17	0.17
MgO	7.24	8.50	6.90	6.32	6.45	7.51	7.34	7.08	7.40	7.39	6.58	6.99	6.81	7.11
CaO	11.75	10.94	11.90	12.98	11.87	12.05	11.94	10.88	11.40	12.66	11.73	12.83	12.49	12.00
Na <sub>2</sub> O	2.11	2.22	2.28	2.26	2.30	2.16	2.31	2.40	2.24	2.11	1.98	2.03	2.05	2.23
K <sub>2</sub> O	0.37	0.29	0.22	0.34	0.42	0.16	0.23	0.20	0.47	0.28	0.51	0.38	0.42	0.25
H <sub>2</sub> O <sub>tot</sub>	3.69	2.44	2.91	2.59	2.87	2.35	2.42	3.77	3.46	2.53	2.49	2.83	2.88	2.77
SO <sub>3</sub>	0.00	0.03	0.02	0.04	0.06	0.04	0.06	0.08	0.03	0.06	0.00	0.03	0.00	0.02
P <sub>2</sub> O <sub>5</sub>	0.08	0.13	0.08	0.08	0.08	0.08	0.08	0.08	0.08	0.08	0.09	0.08	0.10	0.08
Total	99.26	99.00	99.22	99.38	99.55	99.63	99.59	99.19	98.83	98.20	98.65	97.50	98.60	98.81
C.I.P.W. Norms <sup>a</sup>														
Qz	0.00	0.00	0.00	0.27	0.00	0.63	0.00	0.00	0.00	0.00	0.00	0.00	0.00	0.00
Or	2.30	1.78	1.35	2.08	2.58	0.97	1.40	1.24	2.92	1.73	3.15	2.38	2.60	1.54
Ab	18.77	19.47	20.08	19.78	20.20	18.81	20.15	21.33	19.93	18.69	17.50	18.19	18.19	19.68
An	30.23	30.47	33.00	33.60	30.84	32.13	31.39	33.17	30.58	31.07	30.92	30.54	30.22	32.33
Di	24.91	20.17	22.65	26.28	24.33	23.39	23.63	18.63	23.01	27.25	23.99	29.54	27.88	23.67
Hy	13.08	18.31	16.23	11.60	13.42	17.94	16.46	18.57	13.51	11.19	17.56	8.81	10.00	16.17
Ol	4.69	3.60	0.39	0.00	2.39	0.00	0.79	0.54	3.85	3.89	0.83	4.47	5.03	0.36
Mt	3.81	3.80	3.91	3.92	3.85	3.81	3.81	3.96	3.87	3.83	3.82	3.82	3.81	3.89
Il	2.02	2.03	2.15	2.18	2.09	2.05	2.06	2.19	2.08	2.03	2.02	1.99	2.01	2.12
Ap	0.20	0.32	0.20	0.20	0.20	0.20	0.20	0.20	0.20	0.20	0.22	0.20	0.25	0.20
Norm.Plug.An.	61.69	61.01	62.17	62.94	60.42	63.07	60.90	60.86	60.54	62.44	63.86	62.67	62.43	62.16
Diff.Ind.	21.07	21.25	21.43	22.13	22.77	20.41	21.55	22.57	22.85	20.43	20.64	20.57	20.79	21.22
Norm.C.I.	48.71	48.28	45.57	44.26	46.38	47.45	47.05	44.24	46.57	48.49	48.45	48.90	48.99	46.45

Note: Norms are based on analyses recalculated to 100% H<sub>2</sub>O free and with % Fe<sub>2</sub>O<sub>3</sub> standardized at % TiO<sub>2</sub> + 1.5 (Irvine and Baragar, 1971).

TABLE 4  
Trace Elements of Site 337 Basalts (ppm)

	RF 9788	RF 9789	RF 9790	RF 9791	RF 9793	RF 9794	RF 9795	RF 9796	RF 9797	RF 9798	RF 9799	RF 9800	RF 9801	RF 9802
Sr	72	68	74	75	68	77	72	70	68	74	72	73	73	71
Nb	3	<3	<3	<3	3	<3	3	4	<3	<3	5	<3	3	<3
Zr	49	53	53	55	53	57	51	55	53	51	47	52	52	56
Y	28	28	27	31	28	29	28	31	30	25	26	28	30	28
Ni	149	161	151	146	166	266	182	188	179	162	127	163	161	165
Co	51	51	53	65	53	71	57	59	57	54	44	51	50	55
V	301	304	316	328	311	305	312	327	323	309	312	297	309	317
Zn	95	94	96	101	94	97	100	107	94	94	84	92	92	101
Cu	104	82	107	137	102	138	106	85	132	105	94	124	113	103
Cr	478	448	456	459	462	536	446	457	455	464	420	435	454	454
Ce	17	23	14	22	21	5	11	19	22	30	22	17	22	20
Sc	45	46	53	49	46	47	51	50	46	50	44	46	41	46

northern Mid-Atlantic Ridge, with only a mild iron enrichment as indicated in the AFM diagram (see Rashka and Eckhardt, this volume).

### PHYSICAL PROPERTIES

Physical properties include bulk (wet) density and water content, sediment shear strength, unconfined compressive strength, and sonic velocity. Each core section was sampled for water content and syringe density. Shear strength and sonic velocity measurements were made on one section of a homogeneous core, and where lithologic changes were present. Sampling was often limited by large sections of cores which exhibited obvious disturbance. Evolution of gas created void spaces and cracks in the sediment, hence values of GRAPE wet density must be considered to be minimum.

#### Bulk (Wet) Density, Porosity, and Water Content

Figure 6 shows the vertical distribution of bulk density and syringe water content with depth in Cores 1 through 12. Water content remains consistently low in Cores 1 through 4, then increases abruptly in Core 5 to almost double its value in Core 4, and remains high to the base of the section.

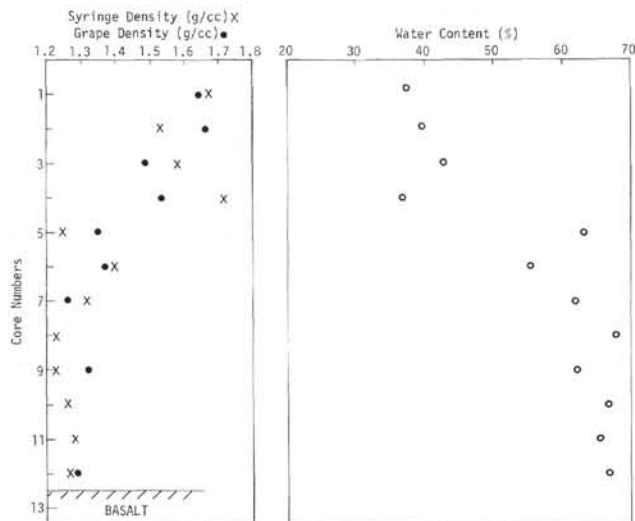


Figure 6. Density and water content profile.

Bulk density presents an inverse picture, being greatest in Cores 1 through 4, and reaching minimum values in Cores 5 through 12. Values shown are corrected GRAPE section values (three per section at 40, 80, and 120 cm intervals), and the syringe wet density (selected at places where shear strength and sonic velocity measurements were made). Correspondence of both techniques appears surprisingly good, particularly in the lower portion of the section where the mean values are identical.

In spite of obvious core disturbance, two distinctly different sedimentary units, possessing different physical properties, are delineated.

#### Shear Strength

Shear strength measurements were made wherever a suitable sedimentary unit was found. A few measurements made in Cores 1 and 2 indicated an increase in strength in the lowest section. These ranged between 0.13 (128.98 g/cc) and 0.16 TSF (158.74 g/cc) and may be considered to represent the strength values in the least-disturbed section of the two cores. Measurements were discontinued through Core 9 due to disturbance (Figure 7).

Penetrometer measurements in Core 10 produced a range of unconfined compression values, from 0.25 (248.07 g/cc) to 1.9 TSF (1.88 kilo/cc). It is not known how much disturbance has affected these values, although disturbance appeared to be minimal.

#### Sonic Velocity-Sediments

Measurements of sonic velocity were made through the split core liner, as the sediments were insufficiently consolidated to measure separately. This resulted in the application of velocity correction factors due to liner thickness. Consequently, individual values within a section may not truly be representative of the sediment sound speed. However, means and standard deviations for each core (where multiple measurements were taken) are shown in Table 5.

#### Summary

Water content and bulk density define two sedimentary units; an upper (density between 1.5-1.7 g/cc; water content between 35%-45%), and lower unit (density between 1.2-1.4 g/cc; water content between 55%-

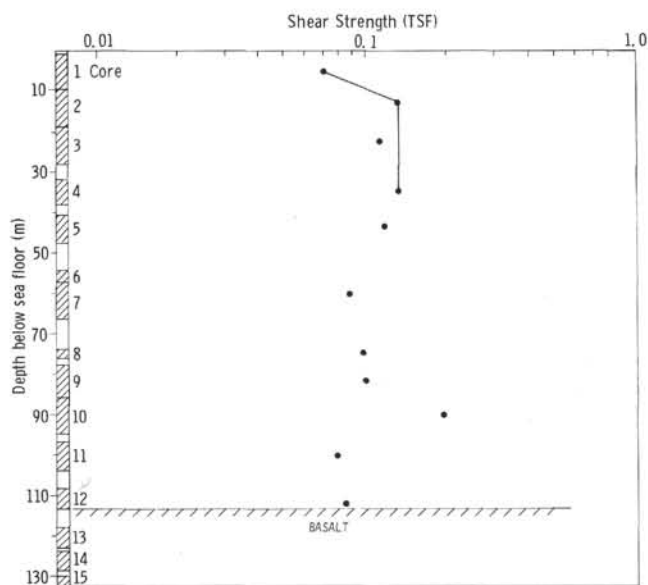


Figure 7. Shear strength profile.

TABLE 5  
Sonic Velocity, Sediments  
From Site 337

Core	Average Velocity (km/sec)	Standard Deviation
1	1.55	—
2	1.54	—
3	1.64	—
4	1.56	—
5	1.61	0.08
6	1.57	0.11
7	1.32	—
8	—	—
9	2.07	—
10	1.54	—
11	2.12	—
12	1.53	—

70%). This zonation may correspond to the Pleistocene/Tertiary boundary.

Shear strength and penetrometer measurements (Figure 7) show a less well defined discontinuity present between Cores 5 and 6, and a relatively homogeneous lower unit between Cores 6 through 12 (broken by a very firm, coherent unit at Core 10).

In view of the above, a perplexing problem is presented in the sonic velocity profile (Figure 8). A major velocity discontinuity is present between Cores 6 and 7 which does not correspond with results shown in either Figures 6 or 7. In addition, the lower unit shows erratic velocity values, the lowest of which is located in Core 12. It is difficult to resolve the high sonic values in Cores 9 and 11, with the low density values in those cores.

It appears that this erratic sonic behavior may be related to the disturbance of the sediments in coring. If so, then the low wet density and high water contents may also be the result of drilling disturbance. The high velocity values may have resulted from measurements

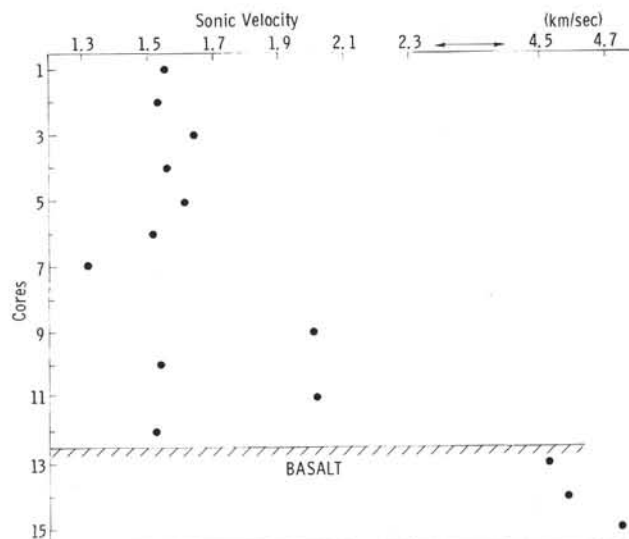


Figure 8. Sonic velocity profile.

made on pebbles and rock chips within the core itself, although this seems unlikely. Whatever the cause, the relationship between sonic velocity, bulk (wet) density, and water content shown at Site 336 cannot be said to be similarly expressed at Site 337.

## GEOCHEMISTRY

### Inorganic Geochemistry

Only three interstitial water samples were taken from the cores of Hole 337. The data are found in Table 6. Analytical methods and procedures are discussed in Chapter 1 (this volume).

### Organic Geochemistry

#### Dissolved Gas in Tertiary Sediments at Site 337

In the course of coring Site 337, a gassy section was encountered beginning at Core 5, and extended to the base of Core 10. Cores 7 and 9 were particularly gassy. Soon after Core 7 was recovered, the polypropylene end cap was forced from the liner, and about 5 cm of mud was extruded as gas pockets began to expand. Within 10 min after the core was recovered, gas pockets were rapidly expanding and could be seen through the liner.

#### Sampling and Analytical Procedure

Gas pockets were always sampled to determine whether methane and other hydrocarbons were present. Gas from all pockets were collected in an evacuated 100-cc can for shore-based isotopic measurements. A rubber septum was attached onto the liner, and a 1-in stainless steel veterinary needle was screwed onto a valve which was welded onto an evacuated can. The needle was pressed into the septum and through the plastic liner, and the gas in the pocket was collected. The septum reduced air contamination and had the added advantage that the same pocket could be sampled several times with little loss of gas through the hole in the liner. Generally when a sample was withdrawn,

TABLE 6  
Summary of Shipboard Geochemical Data, Site 337

Sample (Interval in cm)	Subdepth (m)	pH		Alkalinity (meq/kg)	Salinity (‰)	Ca <sup>++</sup> (mmoles/l)	Mg <sup>++</sup> (mmoles/l)
		Punch-In	Comb.				
Surface Seawater		—	8.33	2.44	34.9	10.34	53.54
1-4, 144-150	6.0	—	8.05	2.81	35.2	10.72	52.41
5-3, 144-150	37.0	—	7.90	2.01	35.2	11.63	52.54
10-5, 144-150	92.5	—	7.35	1.83	35.5	11.94	53.18

the gas pocket in the sediment immediately closed, but in some instances pressure continued to increase and the pocket could be sampled several times.

Composition of the gas samples was determined by means of a portable gas chromatograph designed and constructed by the Exploration and Production Research Division of Phillips Petroleum Company. The chromatograph utilizes a matched pair of 8K thermistors and has two columns which can be switched back and forth for rapid analysis. A 7 ft × ¼ in mole sieve column was used to separate oxygen, nitrogen, and methane. A 20 ft × ¼ in. 20% bisether column on Chromosorb P was used to separate ethane, carbon dioxide, and propane through n-pentane as well as the C<sub>3</sub>-C<sub>5</sub> olefins. Both columns operated at ambient temperatures, and the switching operation required only about 10-15 min for the column to stabilize. Dr. Gordon Spears of British Petroleum Exploration Research kindly provided DSDP with a gas standard on short notice for the shipboard analysis when the Phillips standard was lost in shipment.

In those cases when methane or other hydrocarbons were detected, as a safety precaution subsequent cores were examined for fluorescence with the shipboard fluoroscope.

#### Discussion

Compositional analysis of the gas which formed in the core recovered at Site 337 consists primarily of air with trace quantities of carbon dioxide (Table 7). Neither methane nor any other hydrocarbons were detected in the gas. Apparently the air is introduced during removal of the plastic liner from the core barrel and when the core is cut into sections. Undoubtedly, some air contamination also results when the plastic core liner is pierced in order to obtain a gas sample.

### BIOSTRATIGRAPHY

#### Biostratigraphic Summary

Ice-rafted material is present in Cores 1 to 3 (0-28 m). Well-preserved nannoplankton and foraminiferal assemblages and few radiolarians indicate a Pleistocene age. Reworked Cretaceous and Tertiary nannofossils are present in differing amounts in this sequence, while they are missing in Cores 4 and 5 (28-47 m) of the Pliocene. The Pliocene section is characterized by the presence of *Globigerina atlantica* (sinistral), and a poor nannoplankton assemblage, while siliceous microfossils are missing. Cores 6 to 12 (47-113 m) are barren of calcareous fossils, while diatoms, silicoflagellates, and radiolarians are abundant from Core 9 to Core 12 indicating an early or middle Oligocene age.

TABLE 7  
Shipboard Analysis of Gas Pockets  
in Cores From DSDP Leg 38, Site 337

Sample (Interval in cm)	As Sampled Air	In Liner <sup>a</sup> CO <sub>2</sub>
7-4, 52	99.90	0.1
7-4, 64	99.98	0.02
9-3, 0	99.60	0.4

<sup>a</sup>In mol %.

#### Foraminifera

##### "Glacial," Core 1 through Sample 4-4, 100 cm.

Cores 1 through 3 have a well-preserved to badly corroded planktonic and benthonic foraminiferal fauna. Left coiling (100%-96%) *Neogloboquadrina pachyderma* dominates the planktonic fauna. The only other species observed in the core-catcher samples are *Globigerina bulloides* (1, CC and 2, CC) and *G. quinqueloba* (2, CC). The benthos is a low diversity deep-water association with *Cibicides wuellerstorfi* by far the dominant element. Other species present are: *Quinqueloculina venusta*, *Islandiella teretis*, *Dentalina baggi*, *Marginulina obesa*, *Fissurina* sp., *Cibicides refulgens*, and very rare others. Downward the fauna becomes rare and increasingly shows signs of dissolution. Most samples of Core 3 have mainly fragments, and among the complete specimens the benthonics dominate. All samples of Core 4 (2 in each section) are barren until Sample 4-4, 93-95 cm, the wash residues having a varying amount of ice-rafted material (mainly quartz).

Sample 4-4, 93-95 cm is the lowest sample containing ice-rafted material (very fine quartz and only a few larger grains). Fortunately, it is fossiliferous containing far more than 90% benthonic foraminifera, with *Islandiella teretis* numerically dominant. Other species present are *Cibicides refulgens*, *Cassidulina* sp., *Melonis zaandamae*, and many fragments of these and other species. The planktonic fauna consists of corroded sinistral *Neogloboquadrina pachyderma* in a four-chambered, lobulate morphology. A striking contrast exists between this sample and the one below at 4-4, 116-118 cm. It appears that the base of the "glacial" sequence, as well as the Pleistocene, can be drawn at a level between these two samples.

##### Pliocene, Sample 4-4, 100 cm through Core 5

From Sample 4-4, 116-118 down, the section is free of ice-rafted material. The abundant planktonic foraminiferal fauna is practically monospecific and

made up by the widely variable, sinistral *Neogloboquadrina atlantica*. Rare *Neogloboquadrina pachyderma* and *Globigerina* sp. are found but *Globorotalia* or other planktonic genera are not present. The benthos is somewhat more diverse than the above and has *Cibicides*, *Uvigerina asperual*, *Dentalina baggi*, *Pyrgo murrhina*, *Islandiella teretis*, *Melonis zaandamae*, *Fissurina* sp., *Virgulina* sp., and a few ostracodes.

*Neogloboquadrina atlantica* is often the dominant member of the Pliocene planktonic foraminiferal assemblages in the North Atlantic. Additionally, insofar as age determinations can be made at these sites, *N. atlantica* exhibits a distinct preference for dextral coiling during the late Miocene, has a distinct preference for sinistral coiling during the Pliocene, and has not been identified with certainty in the Quaternary. (Poore and Berggren, 1975).

#### Barren, Cores 6 through 12

Lower in Core 5 dissolution effects become stronger, and in Section 4 the sediments are barren of foraminifera. The wash residues of Cores 6 through 9, Section 5 contain small manganese concretions, but no fossils. The residues of Cores 9 through 12 lack manganese, but contain a few siliceous fossils: radiolarians, sponge spicules, and diatoms.

#### Nannoplankton

Nannoplankton are present in Cores 1 to 5 (0-47 m). Cores 6 to 12 (47-113.5 m) are barren for nannofossils, only siliceous microfossils were found in this sequence. *Emiliania huxleyi*, *Coccolithus pelagicus*, *Gephyrocapsa ericsonii*, and few specimens of *Cyclococcolithus leptoporus* and *Helicosphaera carteri* were observed in Core 1, Section 1 (top) to Sample 1-2, 30-31 cm indicating the *Emiliania huxleyi* Zone (NN 21).

In Sample 1-2, 104-105 cm to Sample 3, CC *Coccolithus pelagicus*, *Gephyrocapsa ericsonii*, and few specimens of *Syracosphaera pulchra*, *Cyclococcolithus leptoporus*, *Discolithina japonica* and *Helicosphaera carteri* are present. Some nannofossil ooze layers in Cores 4 and 5, Section 2 consist only of *Coccolithus pelagicus* and/or *Gephyrocapsa* sp. Within these layers many coccospheres were observed. Nannofossils are generally well preserved, they are slightly etched only in some samples. Reworked Cretaceous and Eocene species were found in Core 1 to Core 3, Section 8. They are rare in the uppermost part of Core 1, but they are more frequent in the lower part of this core. Some samples from Cores 2 and 3 are abundant in reworked species, while autochthonous nannofossils are nearly absent in these samples.

In the interval of Sample 5-2, 97-98 cm to Sample 5-4, 22-23 *Coccolithus pelagicus*, *Reticulofenestra pseudoubilica*, and few specimens of *Cyclococcolithus leptoporus* and *Cyclococcolithus macintyeri* were observed. These species indicate a middle Miocene to early Pliocene age. It is not possible to give a more exact age determination due to the absence of index fossils (discoasters, ceratoliths, sphenoliths).

#### Diatoms (H.-J.S.)

Marine diatom assemblages were only found in the interval between Samples 9-5, 100 cm and 11-2, 10 cm and are common to abundant with moderately to well

preserved tests. The occurrence of *Navicula udintsevii*, *Rouxia obesa*, *Huttonia norwegica*, and *Asterolampra punctifera* places this interval into the *Coscinodiscus oblongus* Zone and is of late Eocene age. No diatoms were found in the "glacial" sequence. Displaced freshwater diatoms were found in Sample 10-5, 120-122 cm and displaced littoral species in Samples 9-5, 100 cm and 10-5, 120 cm.

#### Radiolaria

Based on the radiolarian occurrence, the sediment column can be divided into three units.

Unit 1 (Samples 1, CC through 3, CC) with few to rare radiolarians with a moderate preservation. The faunal assemblage is somewhat similar to the one present in the Norwegian Sea today, but having a lower species diversity, with *Cycladophora davisiana* as the dominant species.

Unit 2 (Samples 4, CC through 7, CC) is characterized by being barren of any siliceous microfossils.

Unit 3 (Samples 9, CC through 11, CC) is characterized by a well-preserved radiolarian fauna, however the species diversity is low. Using Site 338 as a reference, the species assemblage differs somewhat *Lithomitra* sp. A, which was not observed in Site 338, either in the Oligocene or Eocene sediments, indicates an Oligocene age for this unit. It is stratigraphically below the Oligocene recovered from Site 338.

#### Silicoflagellates

Samples from the upper part of this hole are barren for silicoflagellates. The assemblage observed from Sample 9-4, 140-141 cm to Sample 12, CC (81.5-113.5 m) consists of *Corbisema triacantha*, *Distephanus crux*, *Distephanus speculum*, *Naviculopsis biapiculata*, *Naviculopsis ponticula*, *Cannopilus hemisphaericus*, *Dictyocha* cf. *fibula*, *Dictyocha frenguelli*, and *Corbisema apiculata* belonging to the *Naviculopsis biapiculata* Zone which includes the uppermost Eocene, lower and middle Oligocene.

#### Palynology (S.B.M.)

All samples are unproductive, except for trace cysts in one "glacial" sample (Core 1, Section 2).

#### Sedimentation Rates

Because of the scarcity of dated levels, only very rough estimates can be given. The assumption that the base of the "glacial" sediments lies in the middle part of Core 4 (32 m), plus the assumption that such a level is 3 m.y. old, gives an average rate of sediment accumulation of about 1 cm/1000 yr for the upper part of the section. No age is known for the underlying 40 meters of sediments. Using approximately 35 m.y. as a date for the sediment above basement (105 m), the average rate of sediment accumulation of the section below the "glacial" sediments is 0.2 cm/1000 yr. This is a normal rate for pelagic clays and might suggest that a complete section was drilled.

## SUMMARY AND CONCLUSIONS

#### General

Site 337 lies on top of the rift mountains on the east side of the extinct rift valley in the Norway Basin. The

site lies on top of a basement peak, although subsequent sedimentation has made the topography relatively flat. The distance of the site from the axis of the rift is about 20 km.

The drill hole penetrated 132.5 meters of which 113 meters were in sediments, and the remainder in basement. The dominant component of the sedimentary material appears to be pelagic.

In comparing the depth to basement obtained by drilling to that obtained acoustically, the first six cores, that is, the first 56.5 meters, were considered, as a lithologic unit with an average velocity of 1.57 km/sec. The next six cores, that is, the material from 56.5 meters to 113 meters, were treated individually. Velocities ranged from 1.32 to 1.96 km/sec. The calculation yielded a travel time to basement equal to 0.14 sec. Depth to basement is unclear on the seismic record because the bubble pulse runs into basement. It appears that basement is less than 0.18 sec in two-way travel time which is not in conflict with the above calculation.

The Tertiary is nearly coincident with lithologic unit 2, which is an almost complete pelagic accumulation of clays and muds. Below Core 5, the Tertiary is poor in calcareous fossils, being almost completely barren in them below Core 6. Siliceous fossils are barren in Cores 5 through 7, but below Core 8 they increase.

Volcanic ash zones and zeolite clay zones indicate substantial volcanic contributions during the Tertiary. The water content is high and the bulk density is low in the Tertiary compared to the Quaternary section. The velocity values are also lower down to Core 7, below which the measurements appear to give erratic values.

CO<sub>2</sub> was found in Cores 7 and 9, although these gases may also be present in smaller quantities above and below these cores. It is speculated that these gases are products of diagenesis within the Tertiary sediments.

#### Rate of Sedimentation

The sedimentation accumulation rate was high in the "glacial" and lower during the Tertiary. About 32 meters of sediments were deposited during the last 3 m.y. which gives a rate of about 1 cm/1000 yr.

Ignoring uncertainty in the dates for the sediments, and assuming that no part of the sedimentary column is missing, the sediment below the "glacial" section yields an average accumulation rate of about 0.2 cm/1000 yr.

#### Basement

The basement consists of basalt very similar to tholeiitic basalt typically found in mid-ocean ridge rifts. Brecciated layers suggest the presence of 13-14 flows of pillow lavas separated by surfaces with volcanic glass.

The basalt is considerably brecciated and altered. It contains a considerable number of calcite and chlorite veins.

#### Discussion

A principal aim of drilling at Site 337 was to determine the age of basement at the "extinct spreading axis" of the Norway Basin. Radiometric ages determined for basement are  $17.5 \pm 1.5$  m.y. by the Russian group and  $25.5 \pm 2.4$  m.y. by the German Group [Kharin et al., this volume]. From sediments, an age range, from middle Oligocene to Late Eocene (29 m.y. to 43 m.y.) principally on the basis of silicoflagellates is indicated. To reconcile the two kinds of data the youngest paleontological age is tentatively assigned to this site, i.e., 29 m.y.

Site 337 is about 20 km from the "extinct spreading axis." The spreading history is probably quite complicated near the time the axis became extinct. Assuming a half rate of spreading of 0.5 cm/yr, the site is about 4 m.y. younger than the axis, which gives an age of 25 m.y. for the extinct axis. The many assumptions in arriving at this date make it quite tentative.

The details of the history and nature of sedimentation must await further study. A clear implication can be obtained from the fact that the sediments are dominantly pelagic. The site on the extinct rift mountains, even though it has subsided with time, has remained a positive topographic feature and has received no direct inflow of terrigenous sediments.

#### REFERENCES

- Cann, J.R., 1971. Major element variations in ocean floor basalts: Phil. Trans. Roy. Soc. London., v. 268A, p. 494-505.
- Irvine, T.N. and Baragar, W.R.A., 1971. A guide to the chemical classification of the common volcanic rocks. Canadian J. Earth Sci., v. 8, p. 523-548.
- Johnson, G.L. and Heezen, B.C., 1967. Morphology and evolution of the Norwegian-Greenland Sea: Deep-Sea Res., v. 14, p. 755-771.
- LePichon, X., Hyndman, R.D., and Pautot, G., 1971. Geophysical study of the opening of the Labrador Sea: J. Geophys. Res., v. 76, p. 4724-4743.
- Poore, R.Z. and Berggren, W.A., 1975. The morphology and classification of *Neogloboquadrina atlantica* (Berggren): J. Foram. Res., v. 5, p. 76-84.
- Talwani, M. and Eldholm, O., in press. Evolution of the Norwegian-Greenland Sea: Geol. Soc. Am. Bull.
- Vogt, P.R., Ostenso, N.A., and Johnson, G.L., 1970. Magnetic and bathymetric data bearing on sea-floor spreading north of Iceland: J. Geophys. Res., v. 75, p. 903-920.
- Yoder, H.S. Jr., and Tilley, C.E., 1962. Origin of basalt magmas: an experimental study of natural and synthetic rock systems: J. Petrol., v. 3, p. 342-532.



SITE 337		HOLE		CORE 3		CORED INTERVAL: 18.5-28.0m		
AGE	ZONE	FOSSIL CHARACTER				SECTION METERS	LITHOLOGY	LITHOLOGIC DESCRIPTION
		SINUSIAC/OLEN	DIATOMS	SIL FLAG	NANNOPK			
PLEISTOCENE	Gephyrocapsa oceanica (N)					0		<p>Very intense deformation throughout. Colors: olive gray (5Y 3/2), grayish olive (10Y 4/2), moderate olive brown (5Y 4/4), all thoroughly mixed. Clay clasts are present throughout, plus scattered ash, sandy zones.</p> <p><u>MINOR LITHOLOGY</u></p> <p>NANNOFOSSIL OOZE (Smear 5-75)            10% Silt 2-3% Quartz            90% Clay 1% Feldspar            15% Clay minerals            TR- Volcanic glass, Glauconite</p> <p>10Y 4/2            5Y 3/2            5Y 4/4</p> <p>MUD (Smear 6-75)            20% Sand 15% Quartz            40% Silt 5% Feldspar            40% Clay 2% Mica, Zeolites            1% Heavy minerals, Glauconite            4% Opaques            7% Volcanic glass            64% Clay minerals            TR- 2% Foraminifera, Nannofossils</p> <p><u>Carbon-Carbonate (DSDP)</u>            2-110 (0.4, 0.2, 1)</p> <p><u>Grain Size (DSDP)</u>            0-15 (14.3, 41.6, 44.0)            6-70 (24.0, 44.7, 31.3)</p>
		B	B			0.5		
		B/B	B	B		1.0		
		B	B			2		
		B	R/P			3		
		B	B			4		
		B	R/G			5	75	
		B	R/G			6	75	
		B/B	B	B				
		B	A/G					
		B	A/G					
		B	B					
B	R/G							
B	B							
B	B							
B	A/GR/PC/S							
							10Y 4/2, 5Y 3/2, N2	
							10Y 4/2, 5Y 3/2, 5Y 4/4	
							10Y 4/2	
							* CC	

SITE 337		HOLE		CORE 4		CORED INTERVAL: 28.0-37.5m		
AGE	ZONE	FOSSIL CHARACTER				SECTION METERS	LITHOLOGY	LITHOLOGIC DESCRIPTION
		SINUSIAC/OLEN	DIATOMS	SIL FLAG	NANNOPK			
PLIOCENE	Globigerina atlantica (F)					0	VOID	<p>Colors: grayish olive (10Y 4/2), dark greenish-gray (5GY 4/1). Intense deformation with moderate deformation in Sec. 4. Scattered patches of nannofossil ooze, clay fragments, sand.</p> <p><u>MAJOR LITHOLOGIES</u></p> <p>a) Transitional NANNOFOSSIL OOZE (Smears 4-135, CC)            20% Silt 2% Quartz, Opaques            80% Clay 1% Feldspar, Glauconite            5% Volcanic glass            15% Clay minerals            10% Zeolite            3% Carbonate            3% Foraminifera            58% Nannofossils</p> <p>b) MUDS</p> <p><u>MINOR LITHOLOGY</u></p> <p>ASH (Smear 2-75)            80% Sand 5-10% Quartz            10% Silt 5-10% Heavy minerals            10% Clay 0-5% Opaques            0-5% Palagonite            80% Volcanic glass</p> <p><u>Carbon-Carbonate (DSDP)</u>            2-50 (0.2, 0.2, 0)</p> <p><u>Grain Size (DSDP)</u>            2-25 (5.0, 64.8, 30.2)            4-30 (11.1, 40.8, 48.1)</p>
		B/B	B	B		0.5		
		B	B	B		1.0		
		B	B	B		2	75	
		B	B	B		3		
		B	B	B		4		
		B	C/G	B				
		B	A/G					
		B	A/G					
		B	A/G					
		B	B					
		B	A/G					
							10Y 4/2	
							CC	

Explanatory notes in Chapter 1

AGE ZONE	FOSSIL CHARACTER					SECTION METERS	LITHOLOGY	SED. DISTURBANCE	SED. STRUCTURES	LITHO. SAMPLE	LITHOLOGIC DESCRIPTION
	DINOFLAG./SPORE-POLLEN	DIATOMS	SIL. FLAG.	NANNOPLK.	RADIOLARIA						
PLIOCENE	Globigerina atlantica (F)	B/B	B	B	B	B	0				Colors to 4-20: grayish olive (10Y 4/2), greenish-gray (5GY 6/1), dark greenish-gray (5G 4/1), olive gray (5Y 4/1) plus others. 4-20 to 5-150: moderate yellow brown (10YR 5/4), moderate brown (5YR 3/4) plus others in yellows-browns. Intense to moderate deformation; bedding apparent from Sec. 2 down. Local lithified zones, with possible graded beds in Sec. 3, and 2-4 cm bedding in Sec. 4. Contact to Unit 2 at 4-20. Claystone fragments (clasts) present.
							0.5				N7
							1				10Y 4/2
							1.0				5G 6/1
							2				MAJOR LITHOLOGY MUD (Smears 3-80, 5-85, CC) 1% Sand 3- 5% Quartz 15% Silt 2% Feldspar 84% Clay Tr- 5% Heavy minerals 3% Opaques 5- 7% Volcanic glass 5- 7% Zeolites 45-85% Clay minerals 0- 5% Mica
							2				5GY 4/1 5GY 6/1 5GY 4/1 N7
							2				2-4 cm bedding 5G 2/1, 5Y 2/1, 5Y 4/1, 5G 6/1, 5G 4/1
							3				MINOR LITHOLOGIES a) Transitional NANNOFOSSIL Ooze (Smear 3-140) b) ASH (Smear 3-2)
							3				Carbon-Carbonate (DSDP) 2-122 (6.5, 0.1, 53) 4-125 (0.1, 0.0, 1)
							4				Grain Size (DSDP) 1-90 (0.6, 42.6, 56.8) 3-102 (0.2, 28.1, 71.7) 5-50 (0.9, 17.9, 81.3)
							4				10YR 5/4 5YR 3/2 10YR 5/4 5YR 2/2
							5				10YR 6/6
							5				10YR 5/4
							5				5YR 4/4
											CORE CATCHER

AGE ZONE	FOSSIL CHARACTER					SECTION METERS	LITHOLOGY	SED. DISTURBANCE	SED. STRUCTURES	LITHO. SAMPLE	LITHOLOGIC DESCRIPTION
	DINOFLAG./SPORE-POLLEN	DIATOMS	SIL. FLAG.	NANNOPLK.	RADIOLARIA						
							0				Colors: dusky yellow (5Y 6/4), dark yellow orange (10YR 6/6), moderate yellow brown (10YR 5/4). Intense deformation, color mottling, clay. Concretions/clasts.
							0.5				5Y 6/4
							1				10YR 5/4
							1.0				(Hypersthene, amphibole as heavies)
							2				MINOR LITHOLOGY PELAGIC (?) CLAY (Smears 2-85, CC) 10% Silt 5% Quartz 90% Clay 3% Feldspar 6% Heavy minerals 64% Clay minerals 1% Palagonite, Opaques 25% Zeolite 1% Nannofossils
							2				Carbon-Carbonate (DSDP) 2-83 (0.1, 0.1, 0) 2-101 (0.1, 0.0, 0)
							2				Grain Size (DSDP) 1-95 (2.6, 25.7, 71.7)
							2				CORE CATCHER
							2				* CC
							2				

Explanatory notes in Chapter 1





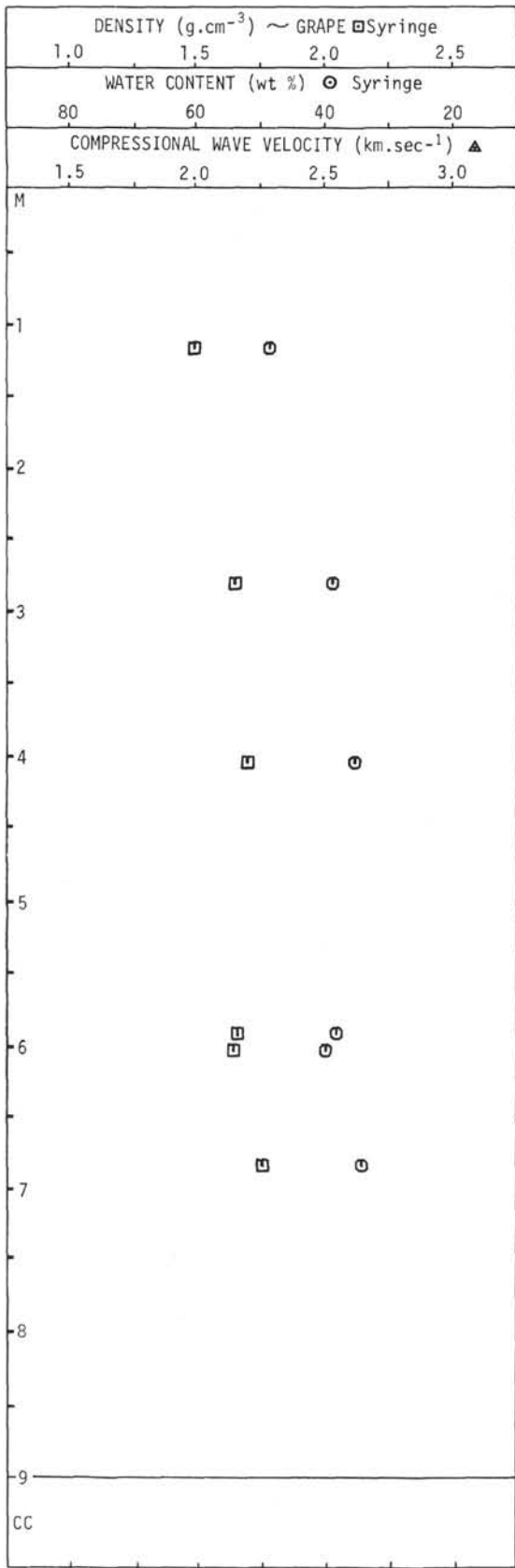


SITE 337		HOLE		CORE 13		CORED INTERVAL: 113.5-123.0 m								
AGE	ZONE	FOSSIL CHARACTER						SECTION	METERS	LITHOLOGY	SED. DISTURBANCE	SED. STRUCTURES	LITHO. SAMPLE	LITHOLOGIC DESCRIPTION
		DINOFLAG./ SPORES-POLLEN	DIATOMS	SIL. FLAG.	NANNOPK.	RADIOLARIA	FORAMINIFERA							
								0		VOID				<u>BASALT</u>  Sec. 1 (60-115 cm) dark gray massive microporphyric, variolitic basalt with abundant, small (1-2 mm) round amygdules of white calcite; (115-150 cm) breccia composed of angular fragments of palagonitized and chloritized glass, basalt fragments cemented by calcite-chlorite-smectite matrix. Thin (1-2 mm) veins of white calcite.  Sec. 2 (0-50 cm) dark gray amygdaloidal aphyric to sparsely phyrlic variolitic basalt. Amygdules (2-3 mm) filled with white calcite and green chlorite-smectite (?); (50-75 cm) amygdaloidal basalt with veins of yellowish calcite with angular fragments of dark-green chlorite; (75-100 cm) breccia; angular fragments altered porous basalt and dark-green chlorite (4-5 cm), cemented by a chlorite-calcite matrix; (100-150 cm) amygdaloidal variobasalt, to massive basalt with calcite veins. Angular fragments of chlorite in veins.  Sec. 3 (0-125 cm) brecciated dark gray aphyric to sparsely phyrlic variolitic basalt, cut by numerous calcite veins with angular fragments of chlorite and palagonite; (125-150 cm) brecciated basalt with calcite amygdules (5%), (1-2 mm).  Sec. 4 (0-75 cm) brecciated dark gray altered aphyric to sparsely phyrlic variolitic basalt with rare amygdules of calcite and numerous calcite-chlorite veins. Angular fragments of basaltic volcanic glass replaced by palagonite and chlorite.
								0.5						
								1						
								1.0						
								2						
								3						
								4		SEDIMENT "OUT OF PLACE"				

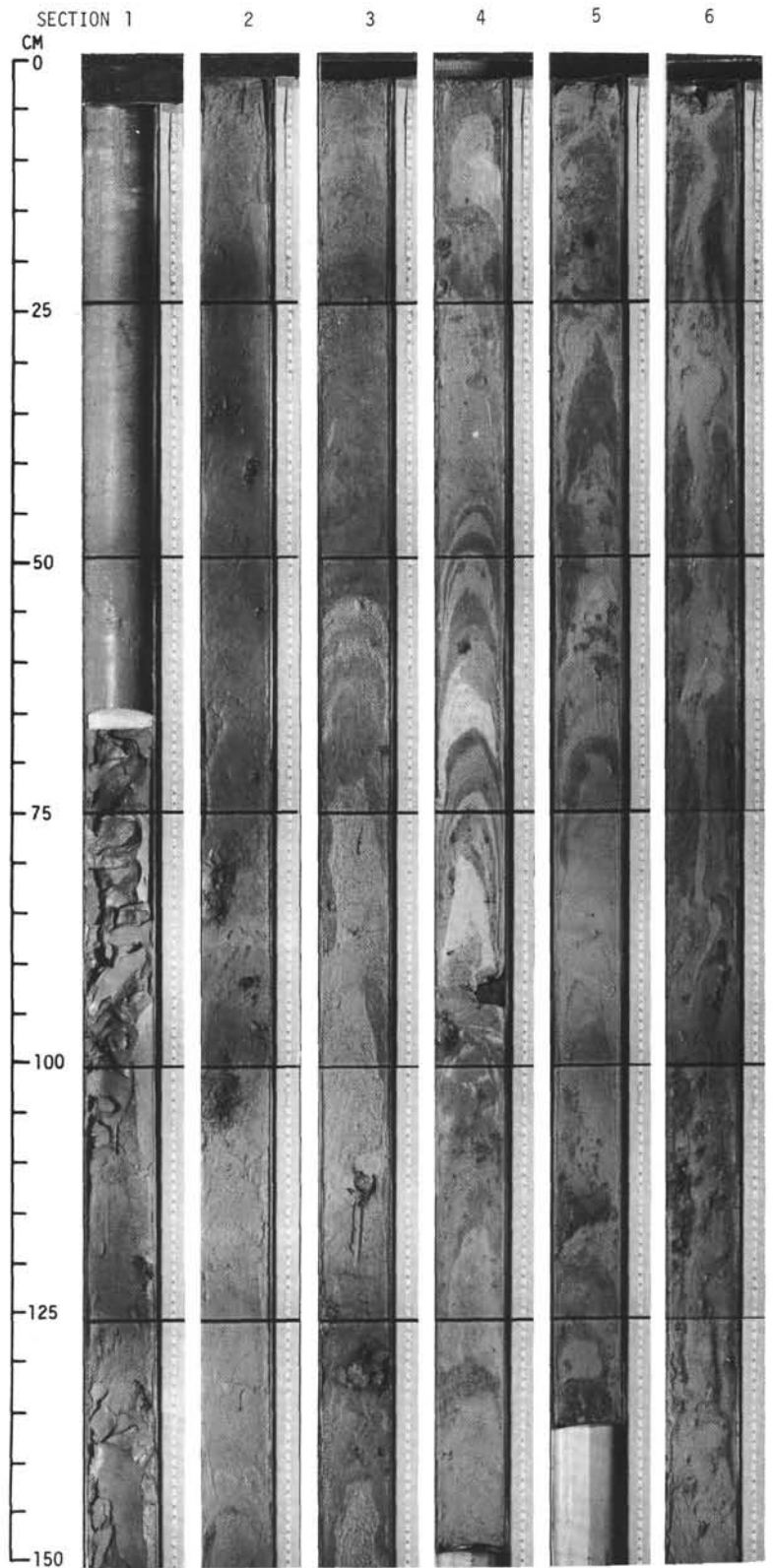
SITE 337		HOLE		CORE 14		CORED INTERVAL: 123.0-128.5 m								
AGE	ZONE	FOSSIL CHARACTER						SECTION	METERS	LITHOLOGY	SED. DISTURBANCE	SED. STRUCTURES	LITHO. SAMPLE	LITHOLOGIC DESCRIPTION
		DINOFLAG./ SPORES-POLLEN	DIATOMS	SIL. FLAG.	NANNOPK.	RADIOLARIA	FORAMINIFERA							
								0		VOID				<u>BASALT/BASALT BRECCIA</u>  Sec. 1 (0-50 cm) breccia composed of angular fragments of basalt and rare palagonite and chlorite; cemented by chlorite-smectite-calcite matrix; (50-150 cm) dark gray brecciated variolitic basalt with white calcite and dark-green chlorite amygdules (to 5%) (1-3 mm). Abundant calcite veins with inclusion of dark-green chlorite. On vein contacts the basalts are lighter (yellow-gray), with some ferruginous material.  Sec. 2 (0-75 cm) brecciated sparsely phyrlic variolitic basalt with rare, empty round vugs. Abundant chlorite-calcite-smectite veins with angular fragments of volcanic basaltic glass replaced by palagonite chlorite and smectite; (75-125 cm) variolitic basalt with olivine phenocrysts replaced by iddingsite. Palagonitized, chloritized, volcanic glass; (125-150 cm) palagonite and chlorite in calcite matrix.  Sec. 3 (0-25 cm) chlorite veins with calcite. Brecciated, ferruginous variolitic basalt; (25-50 cm) palagonitized and chloritized glass. Variolitic basalt with chlorite-calcite-smectite amygdules; (50-75 cm) calcite veins with chlorite; (75-100 cm) palagonitized and chloritized glass; (100-125 cm) aphyric variolitic basalt with chlorite amygdules; (125-150 cm) breccia.
								0.5						
								1						
								1.0						
								2						
								3						

SITE 337		HOLE		CORE 15		CORED INTERVAL: 128.5-132.5 m								
AGE	ZONE	FOSSIL CHARACTER						SECTION	METERS	LITHOLOGY	SED. DISTURBANCE	SED. STRUCTURES	LITHO. SAMPLE	LITHOLOGIC DESCRIPTION
		DINOFLAG./ SPORES-POLLEN	DIATOMS	SIL. FLAG.	NANNOPK.	RADIOLARIA	FORAMINIFERA							
								0		VOID				<u>BASALT/BASALT BRECCIA</u>  Sec. 1 (75-100 cm) basaltic breccia with angular fragments of variolitic basalt and palagonitized glass in smectite-chlorite matrix; (100-140 cm) slightly brecciated variolitic basalt with altered olivine phenocrysts and chlorite-calcite amygdules; (140-150 cm) calcite veins with chlorite.  Sec. 2 (5-50 cm) breccia with angular fragments of palagonitized glass and chlorite in calcite-chlorite-smectite matrix; (50-75 cm) calcite veins; (75-90 cm) breccia; (90-145 cm) amygdaloidal, variolitic basalt with olivine phenocrysts replaced by iddingsite and calcite; (145-150 cm) breccia.
								0.5						
								1						
								1.0						
								2						

Explanatory notes in Chapter 1

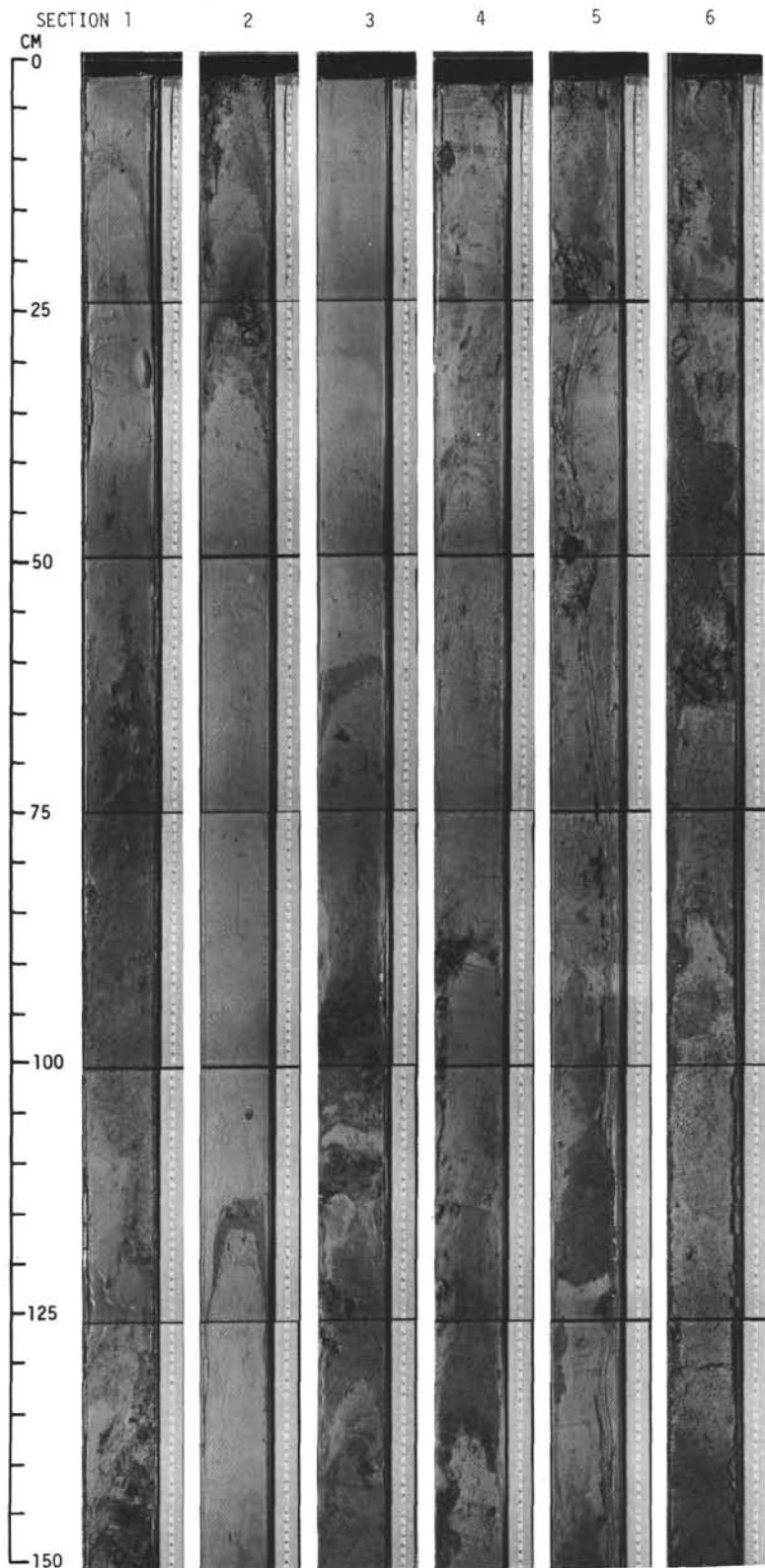
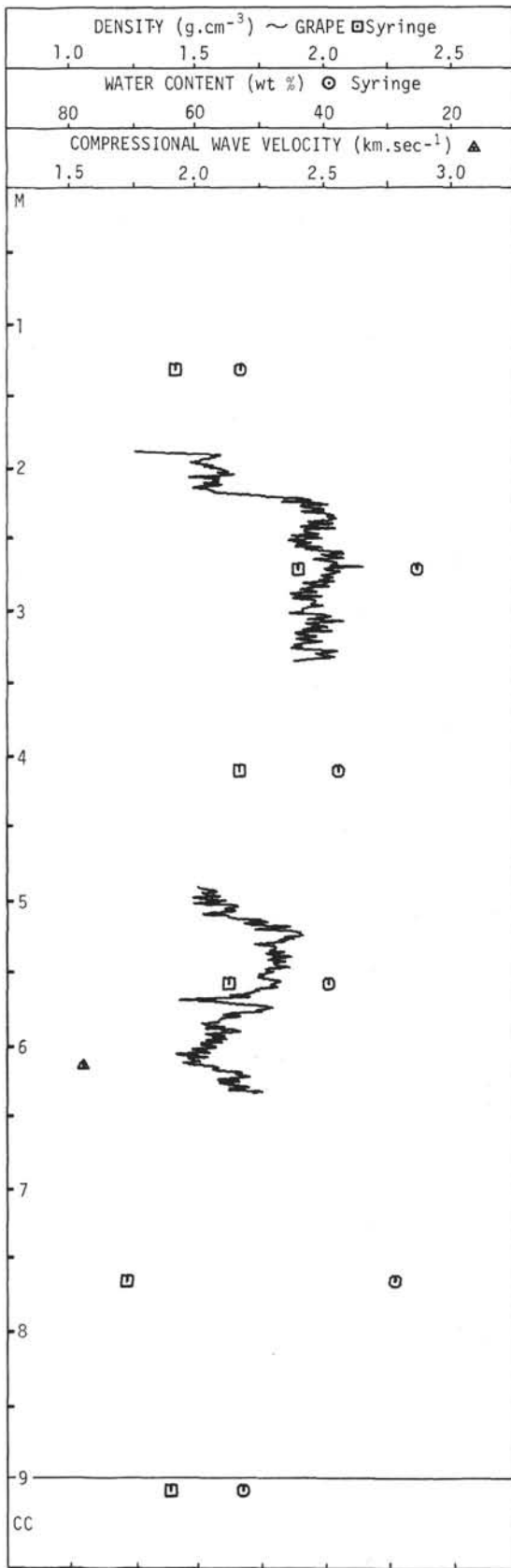


337-1



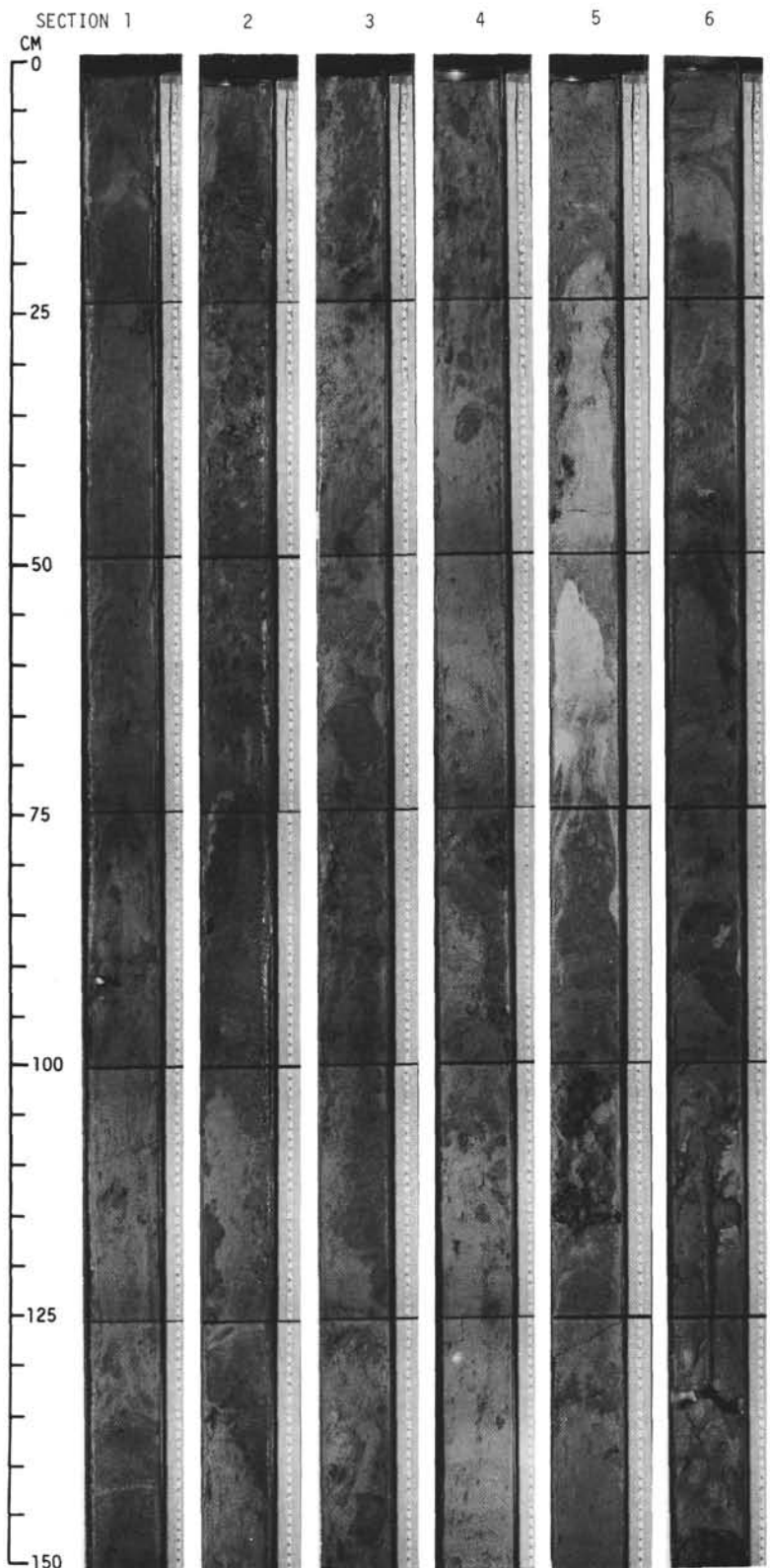
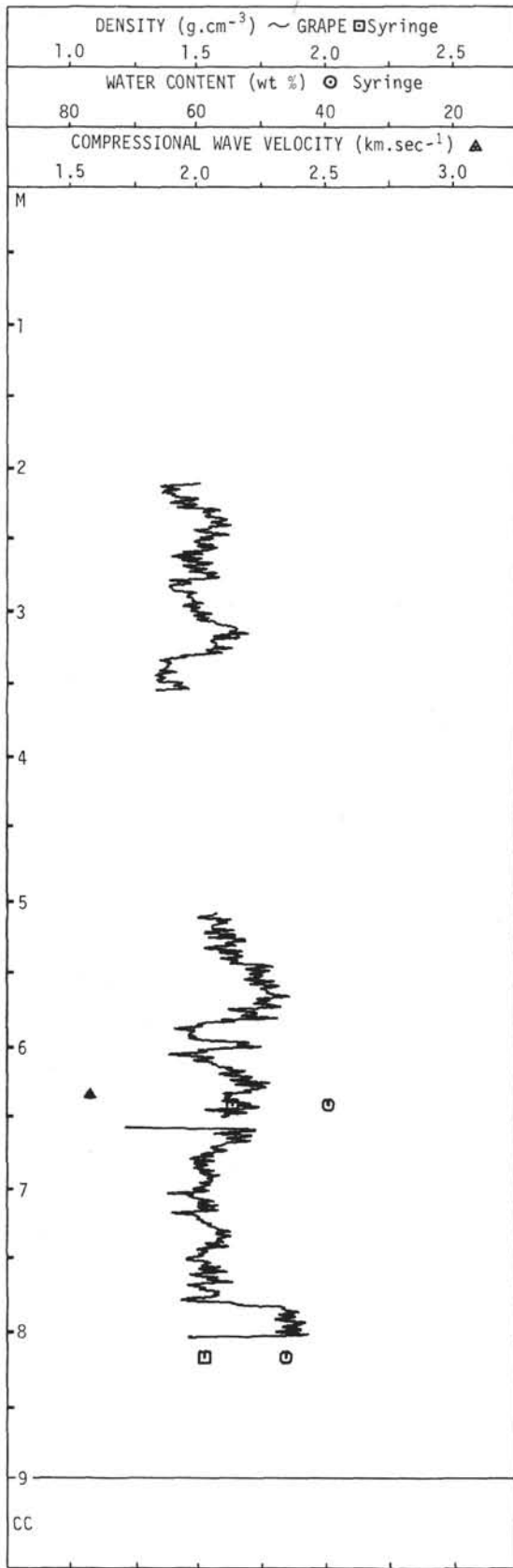
For Explanatory Notes, see Chapter 1

337-2



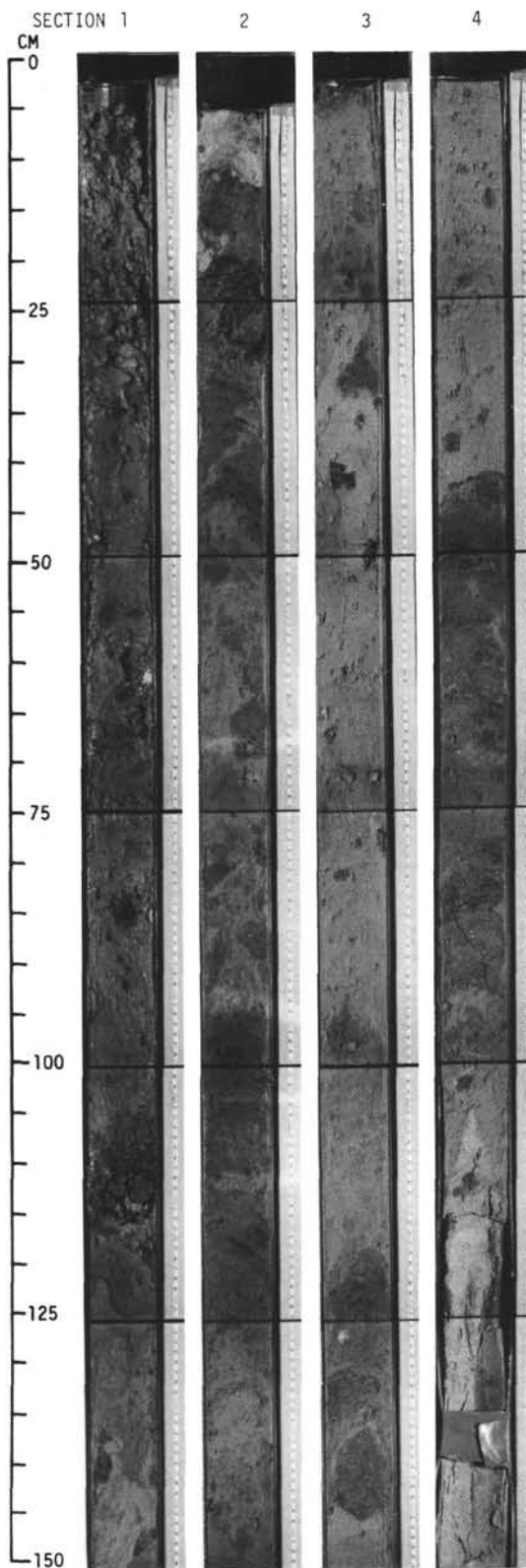
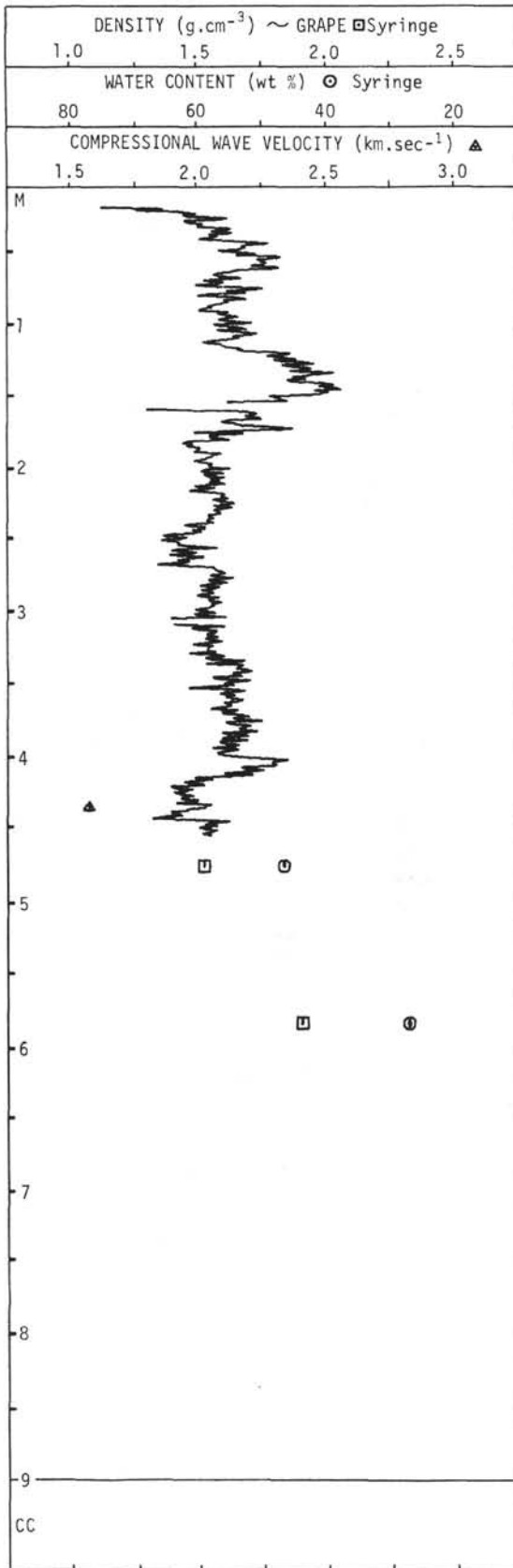
For Explanatory Notes, see Chapter 1

337-3



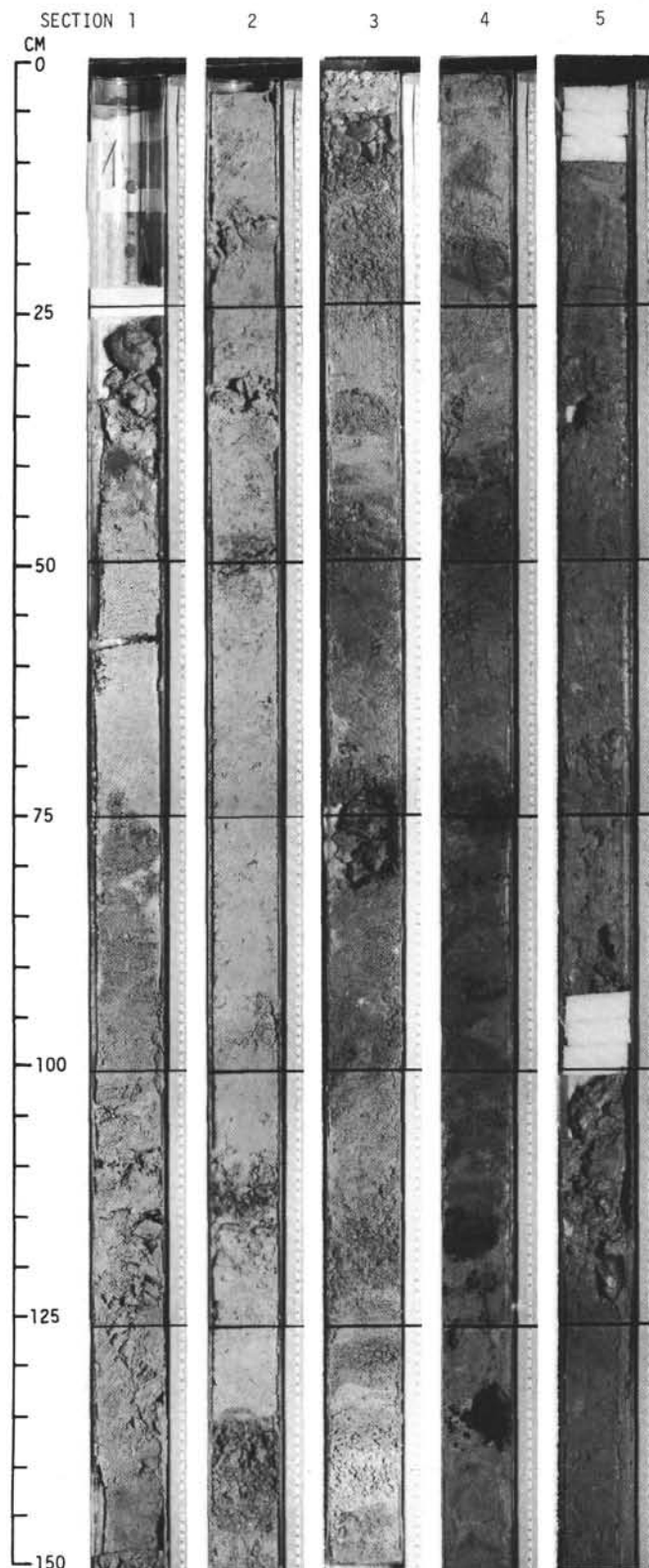
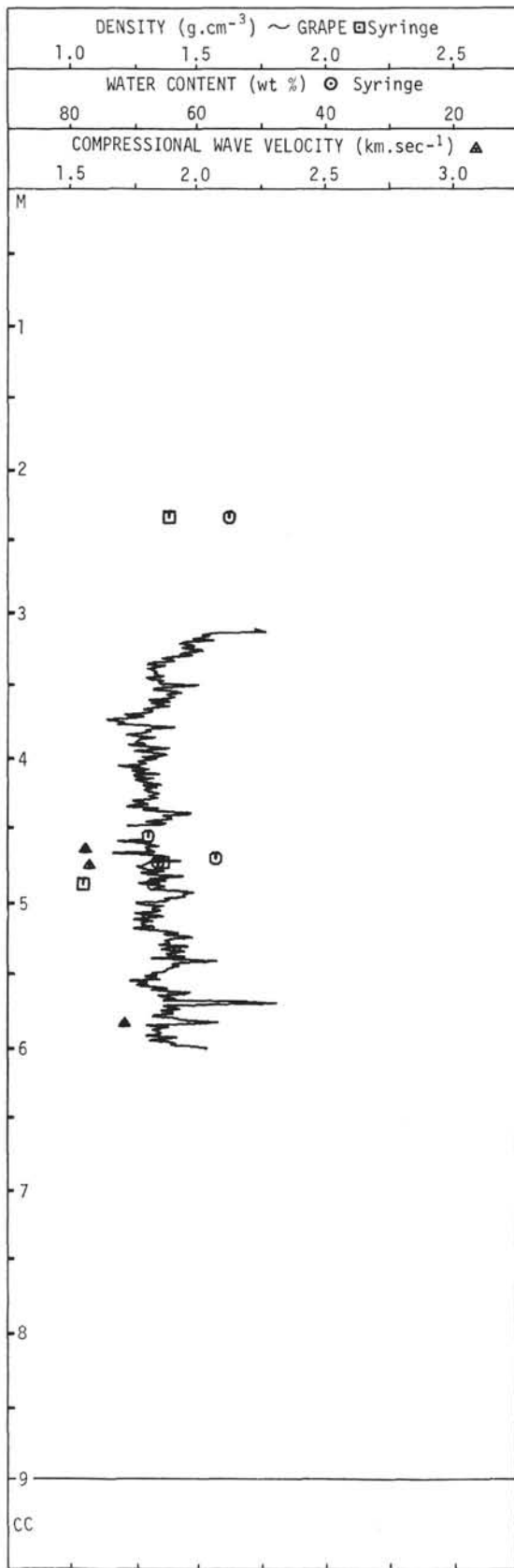
For Explanatory Notes, see Chapter 1

337-4



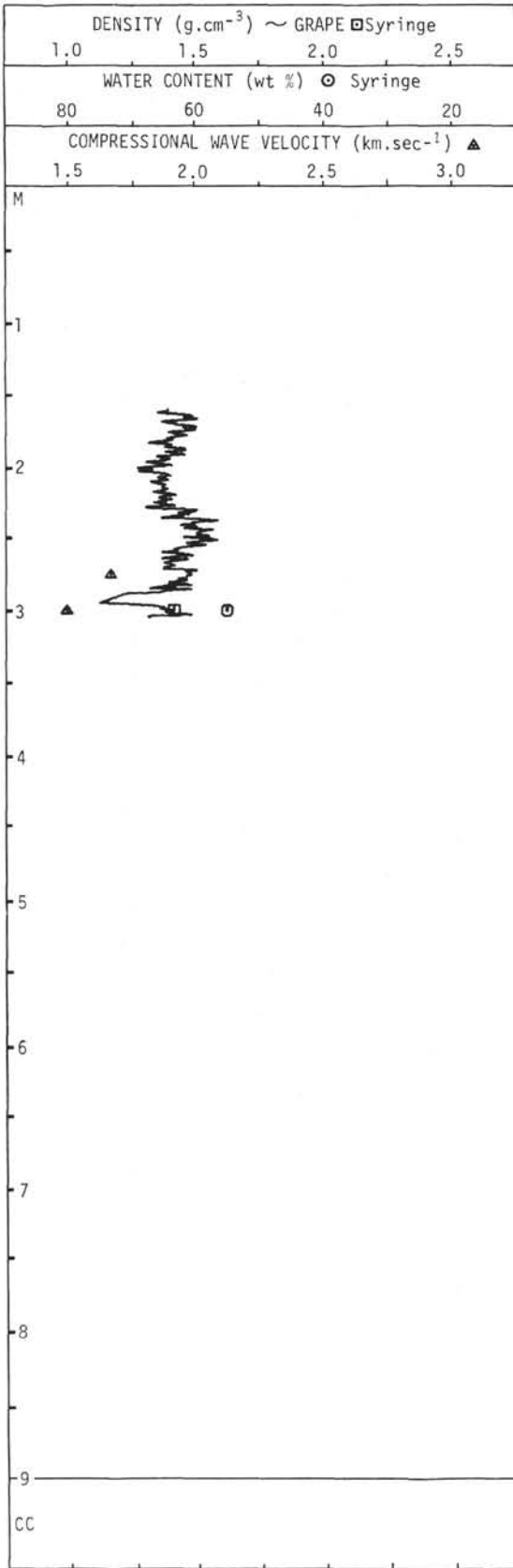
For Explanatory Notes, see Chapter 1

337-5

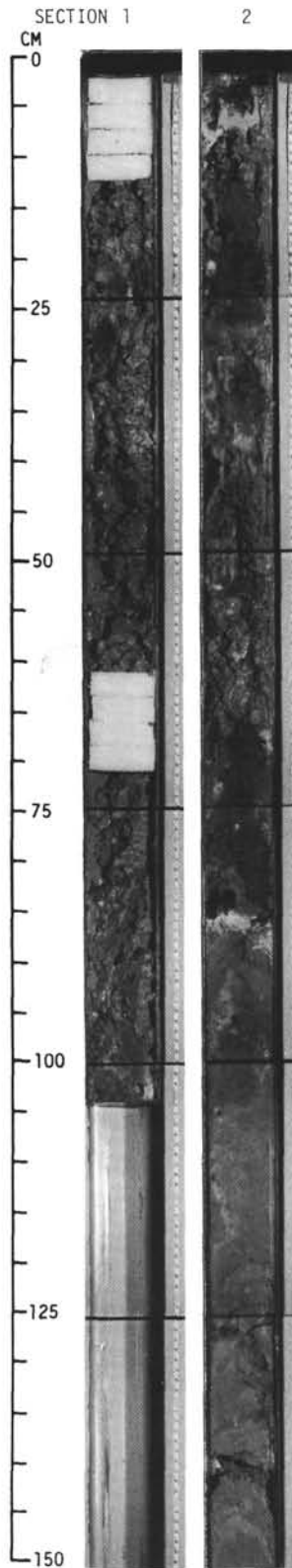


For Explanatory Notes, see Chapter 1

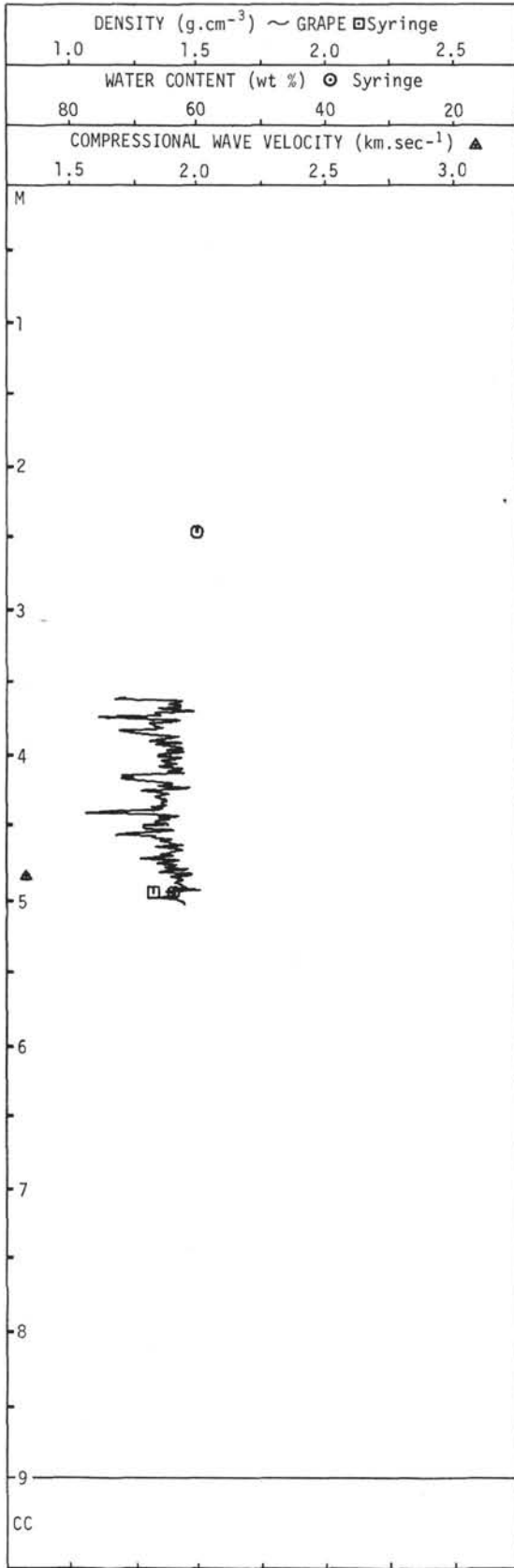
337-6



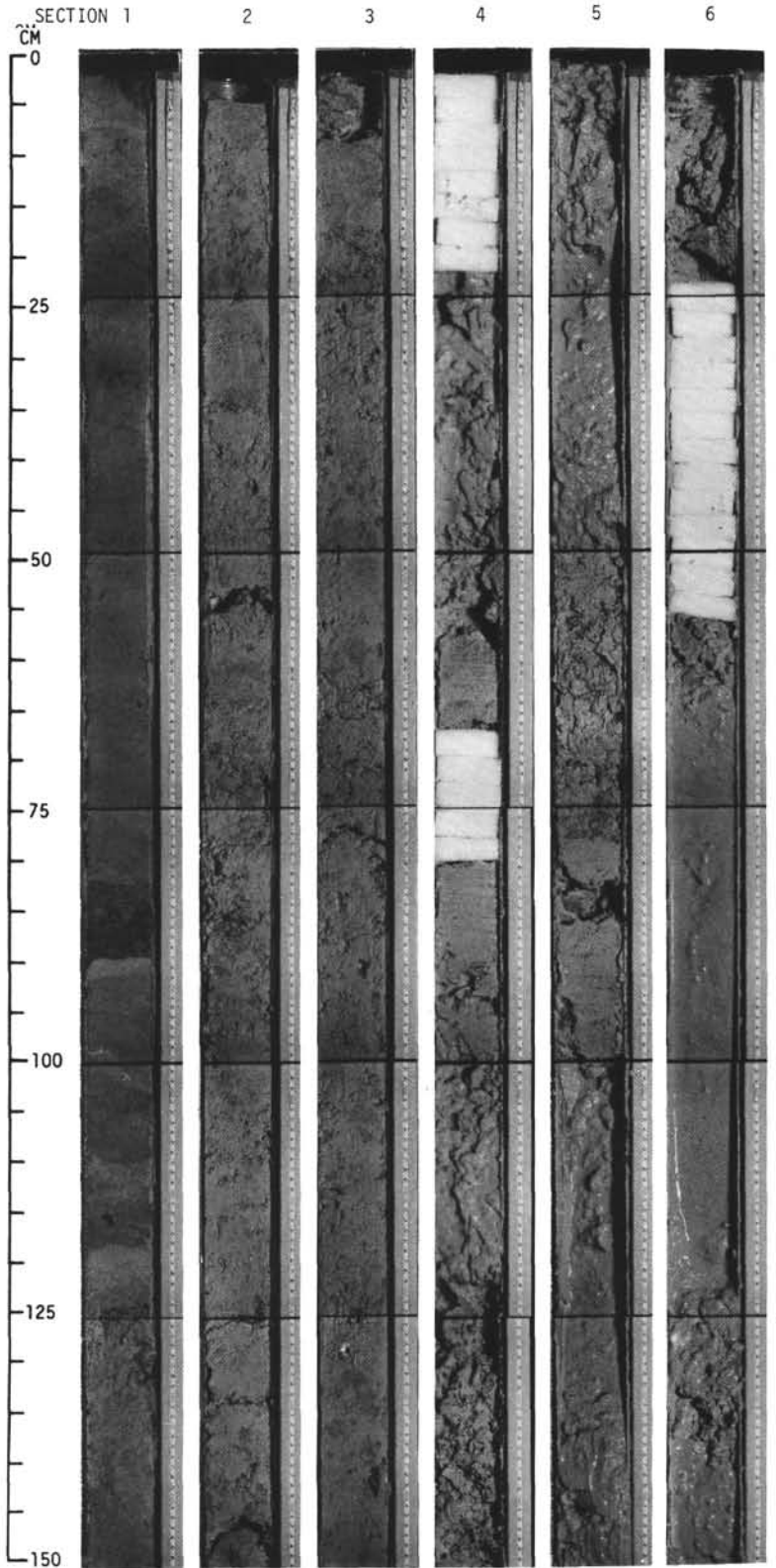
For Explanatory Notes, see Chapter 1

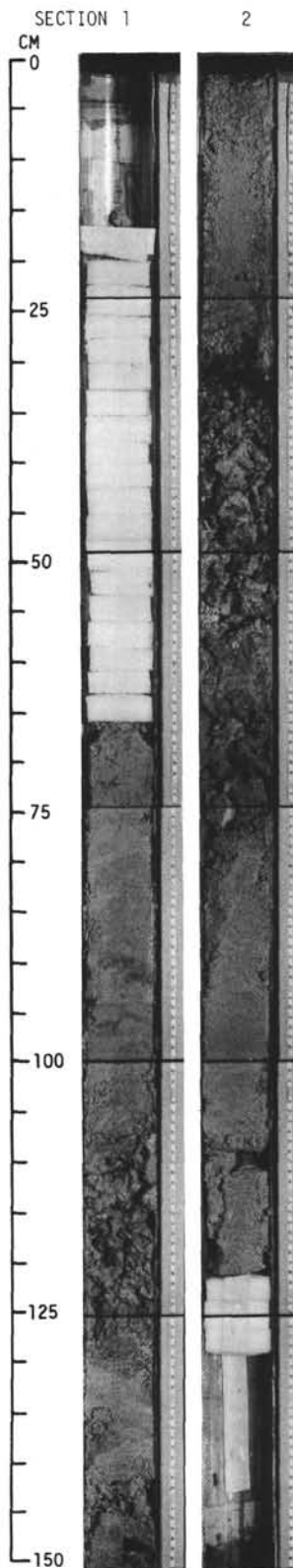
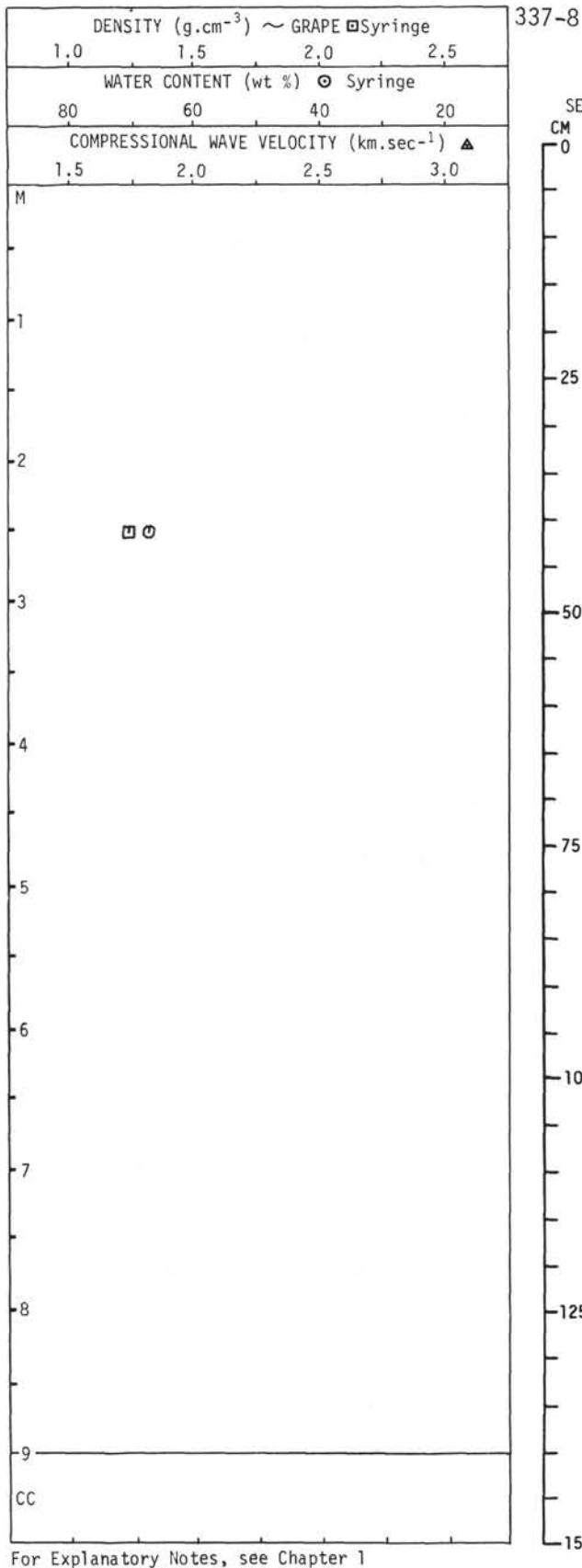


337-7

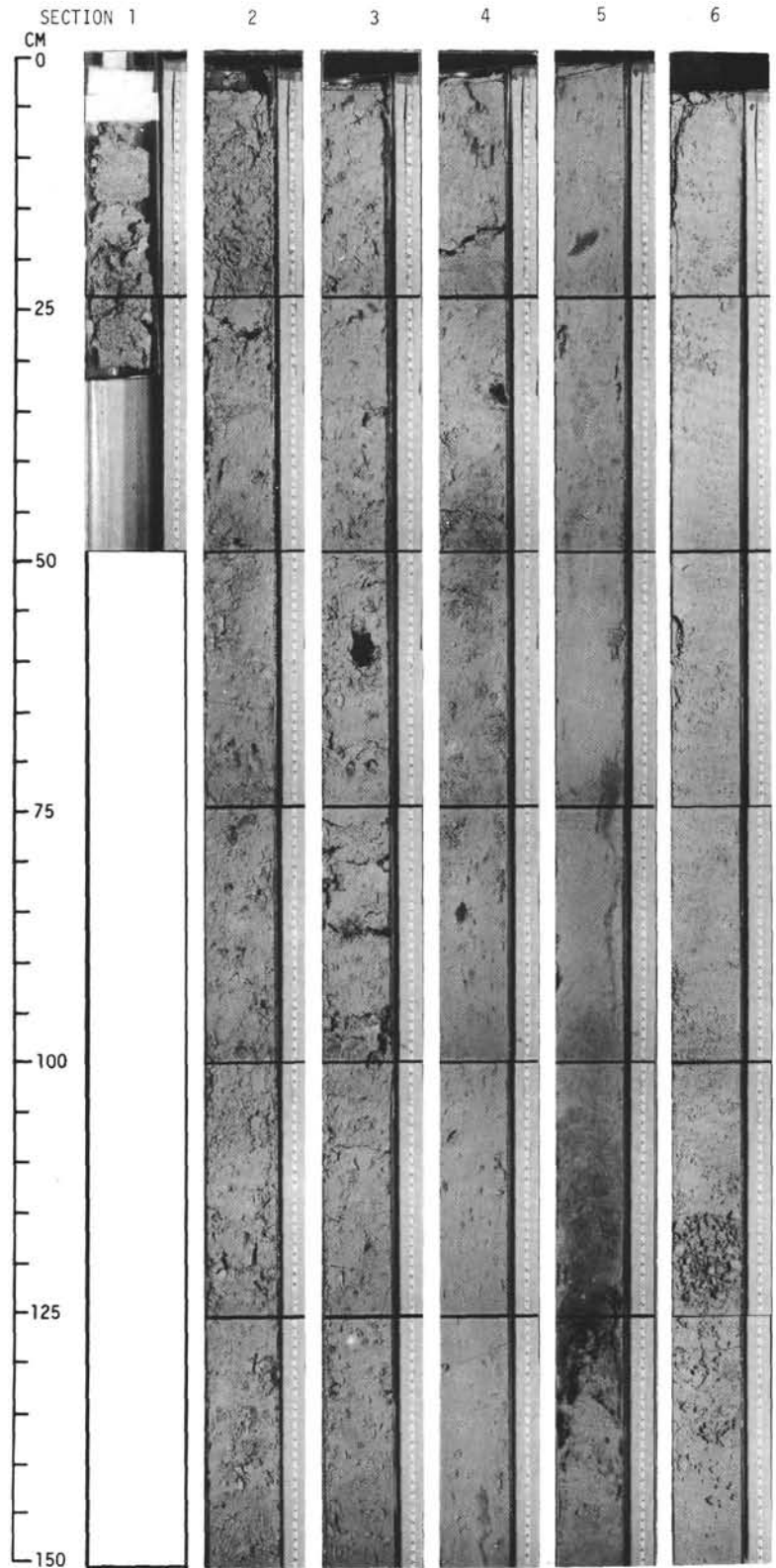
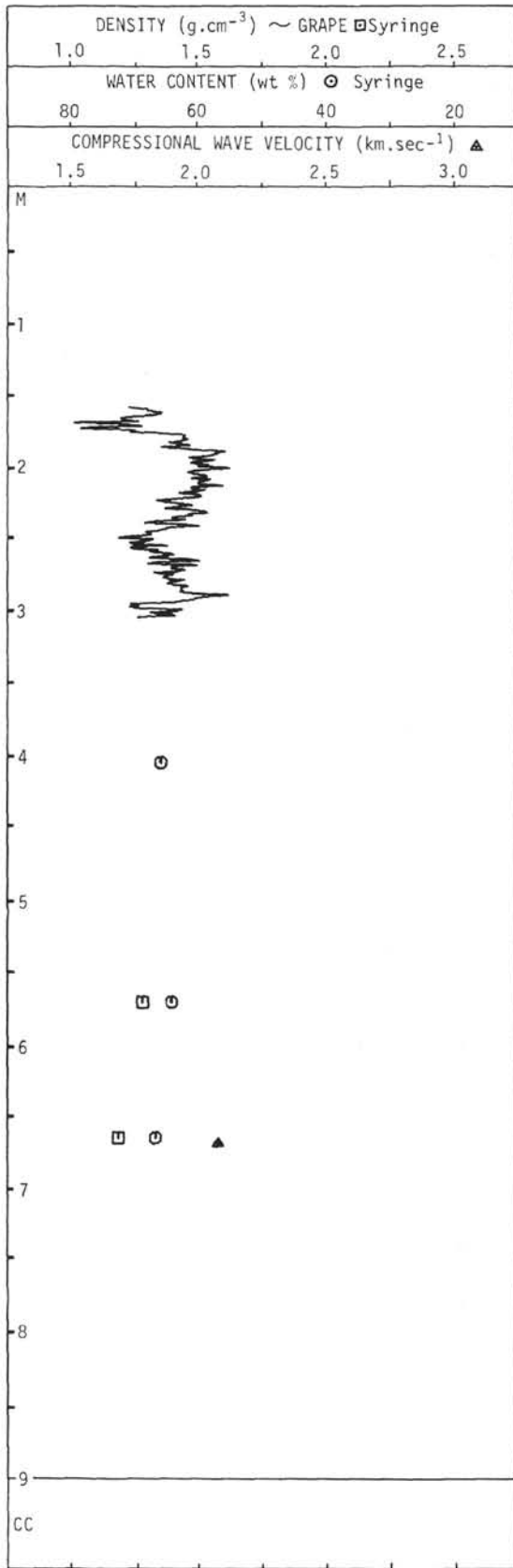


For Explanatory Notes, see Chapter 1



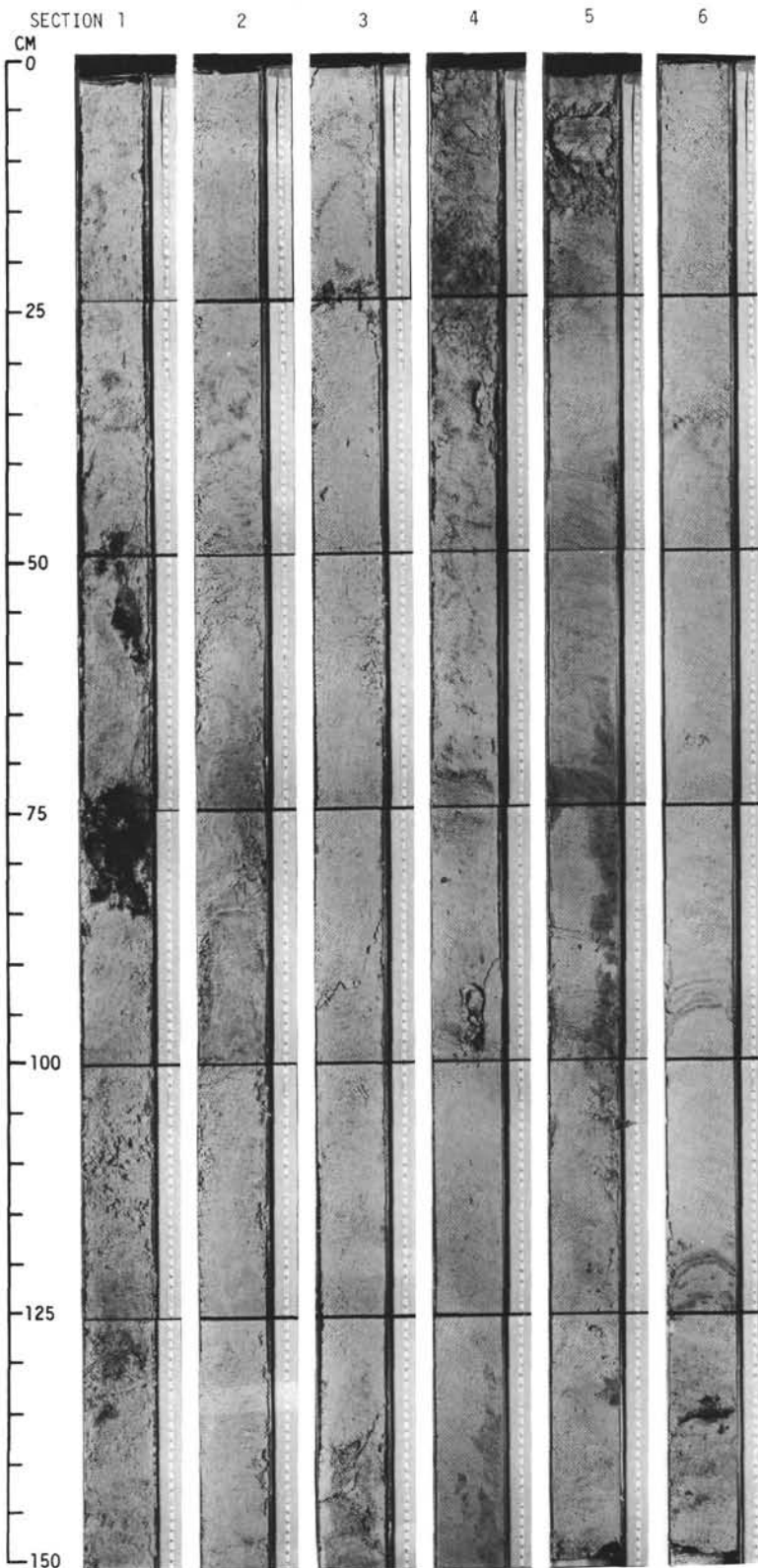
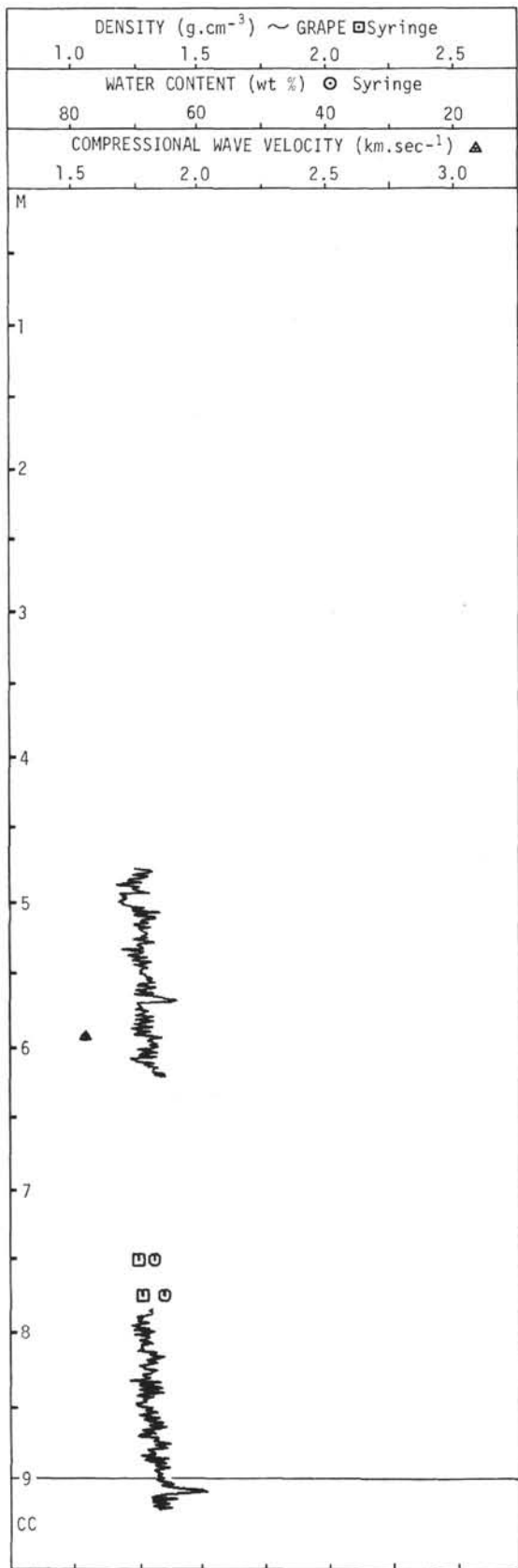


337-9



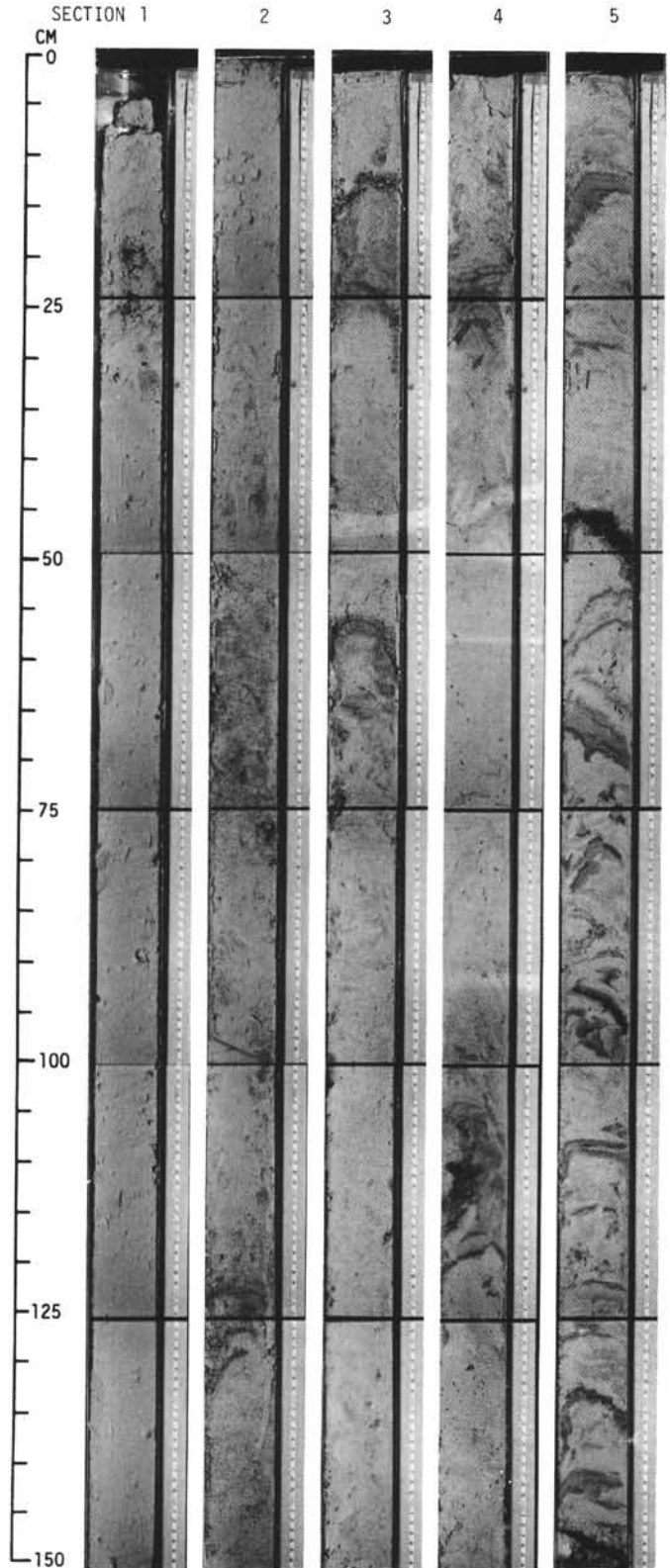
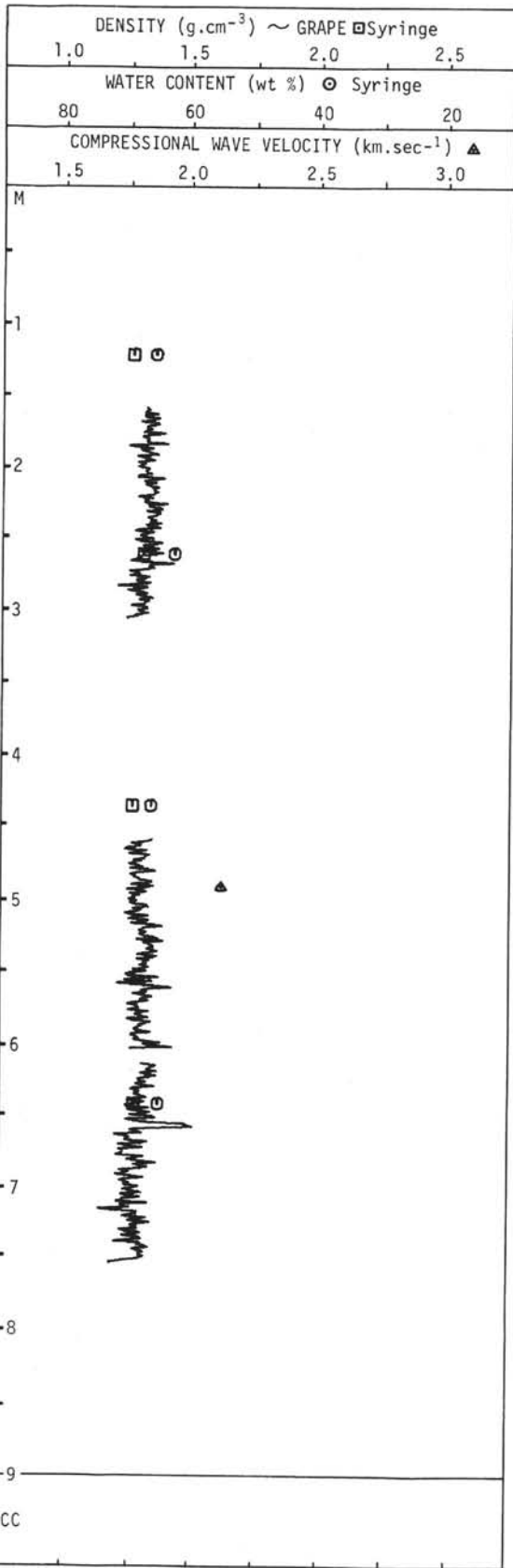
For Explanatory Notes, see Chapter 1

337-10

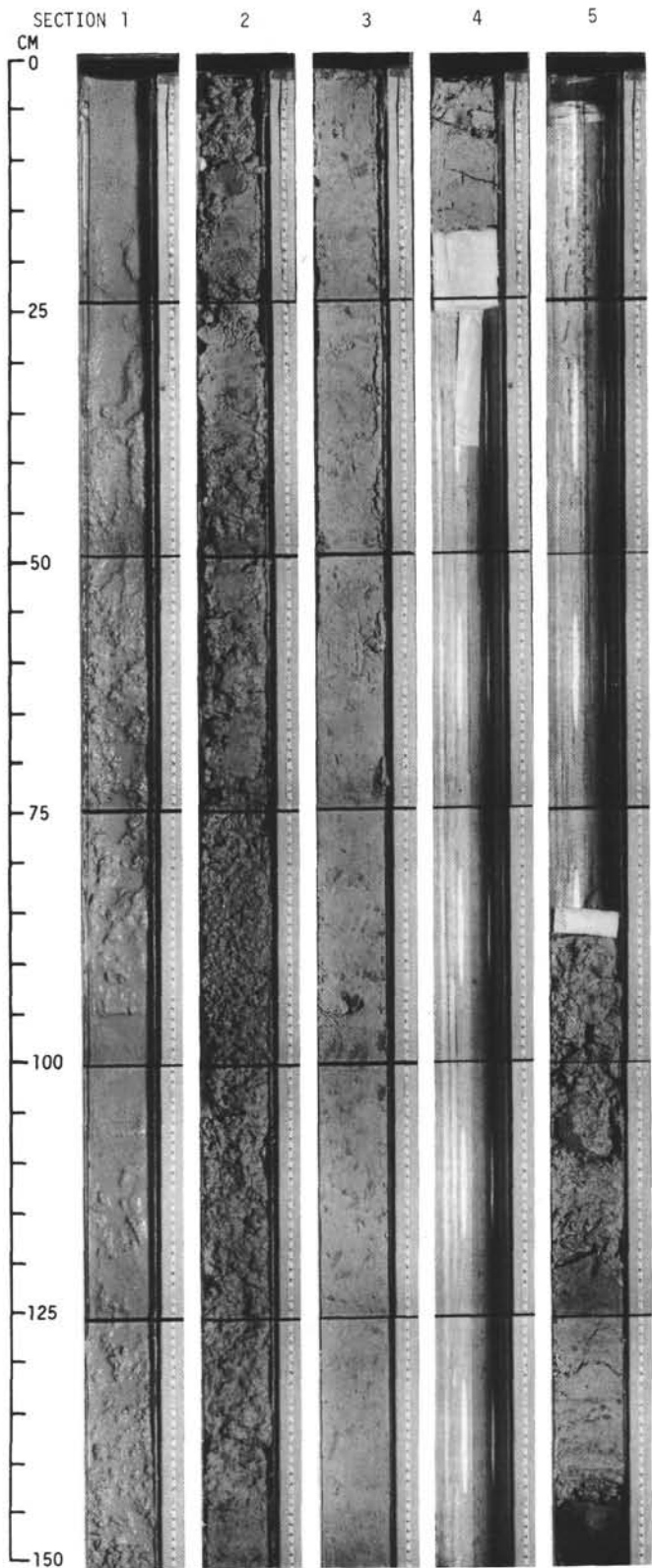
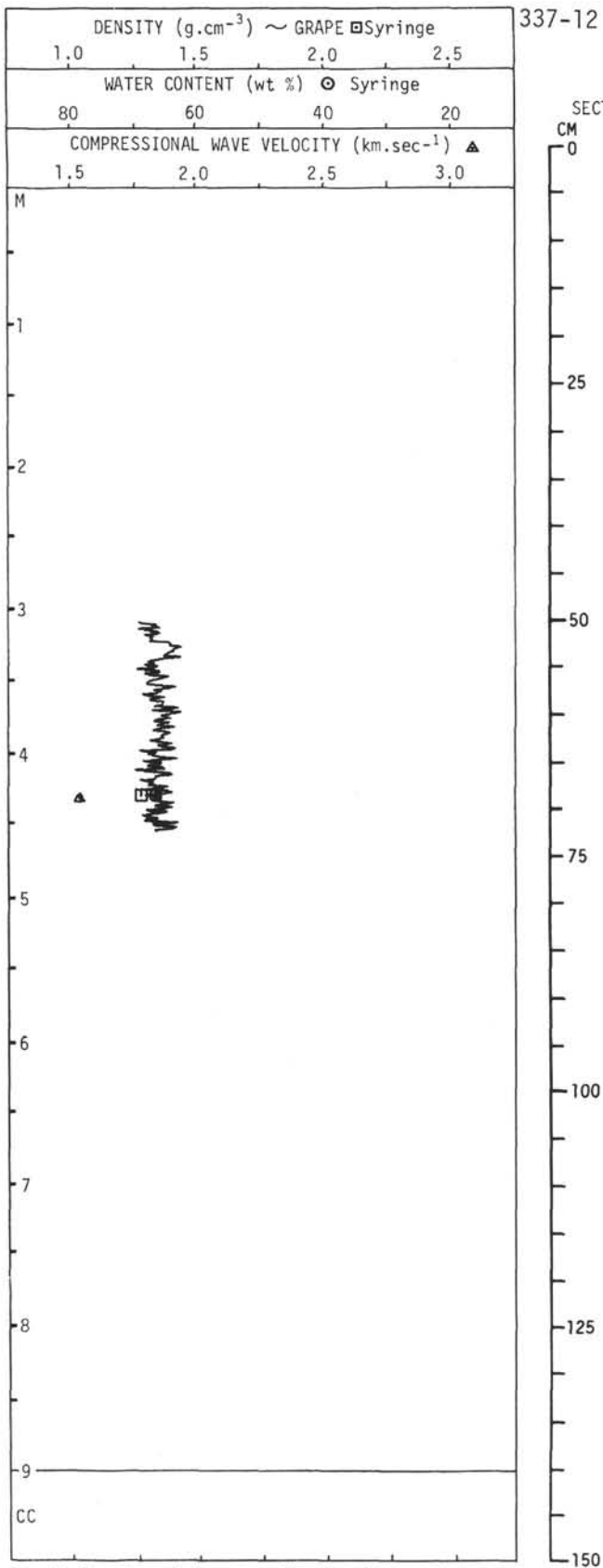


For Explanatory Notes, see Chapter 1

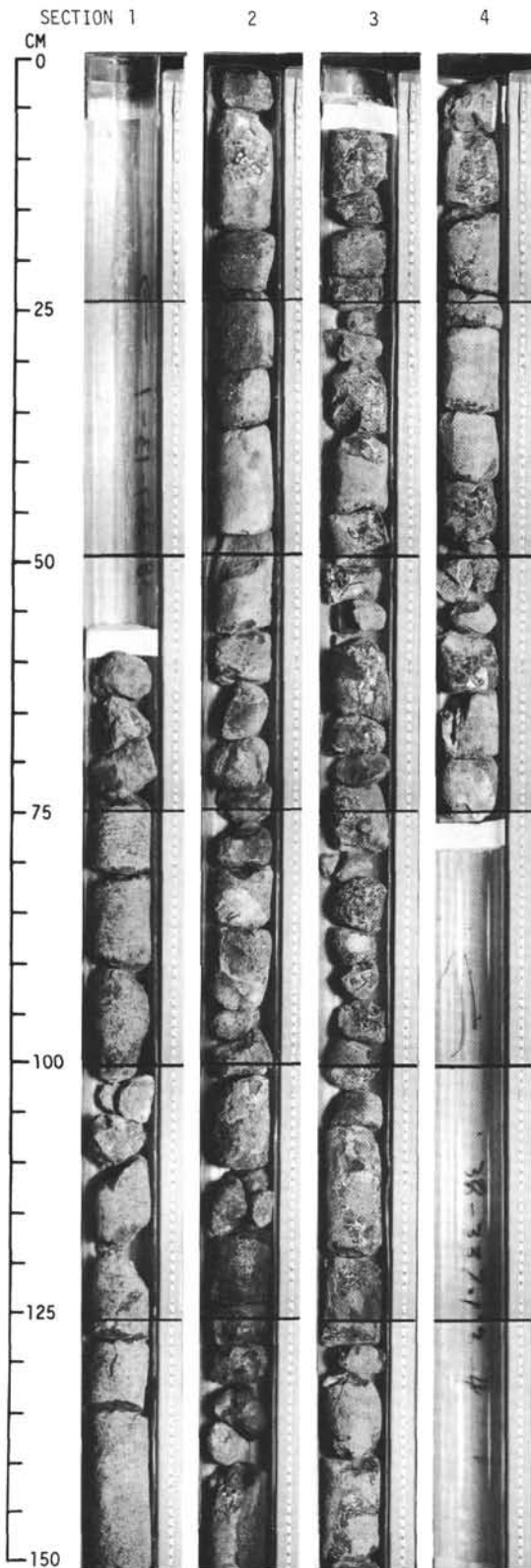
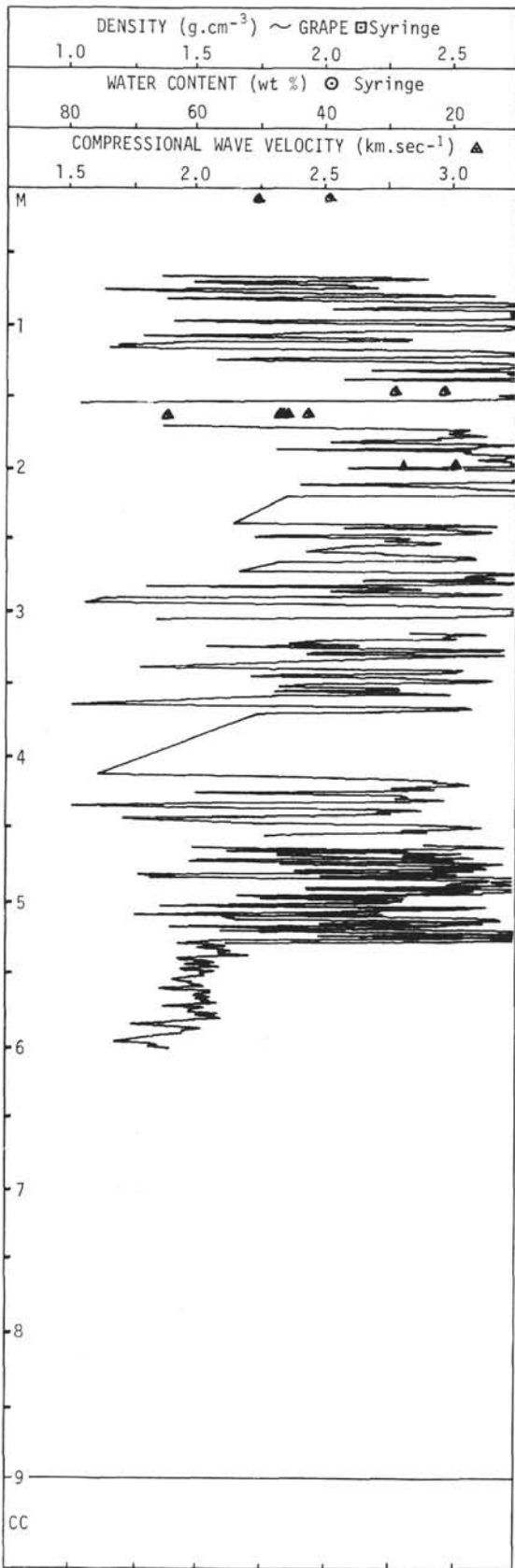
337-11



For Explanatory Notes, see Chapter 1

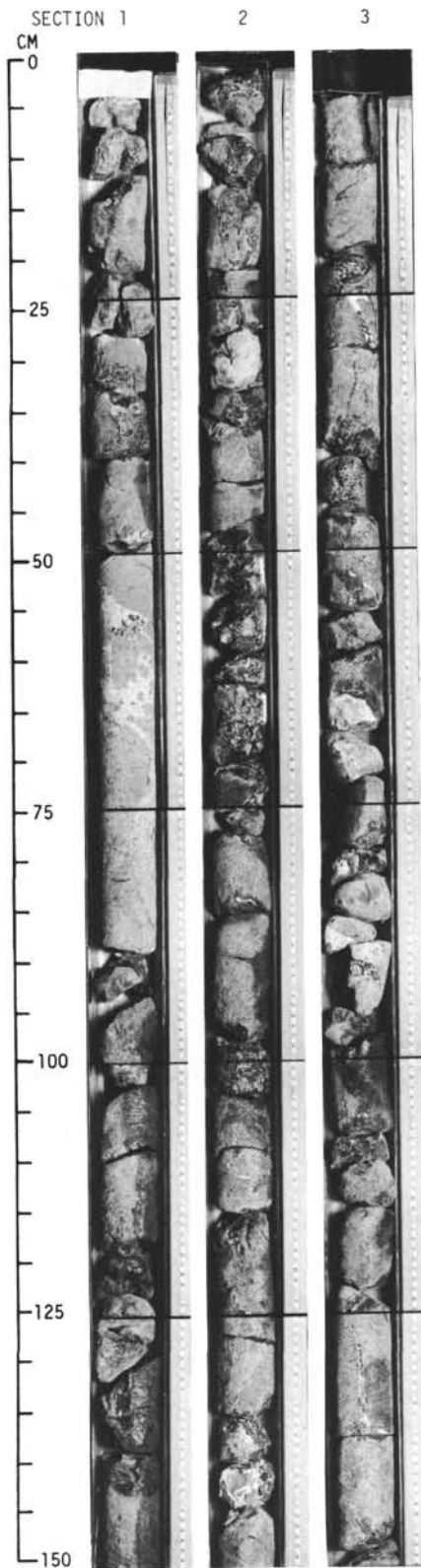
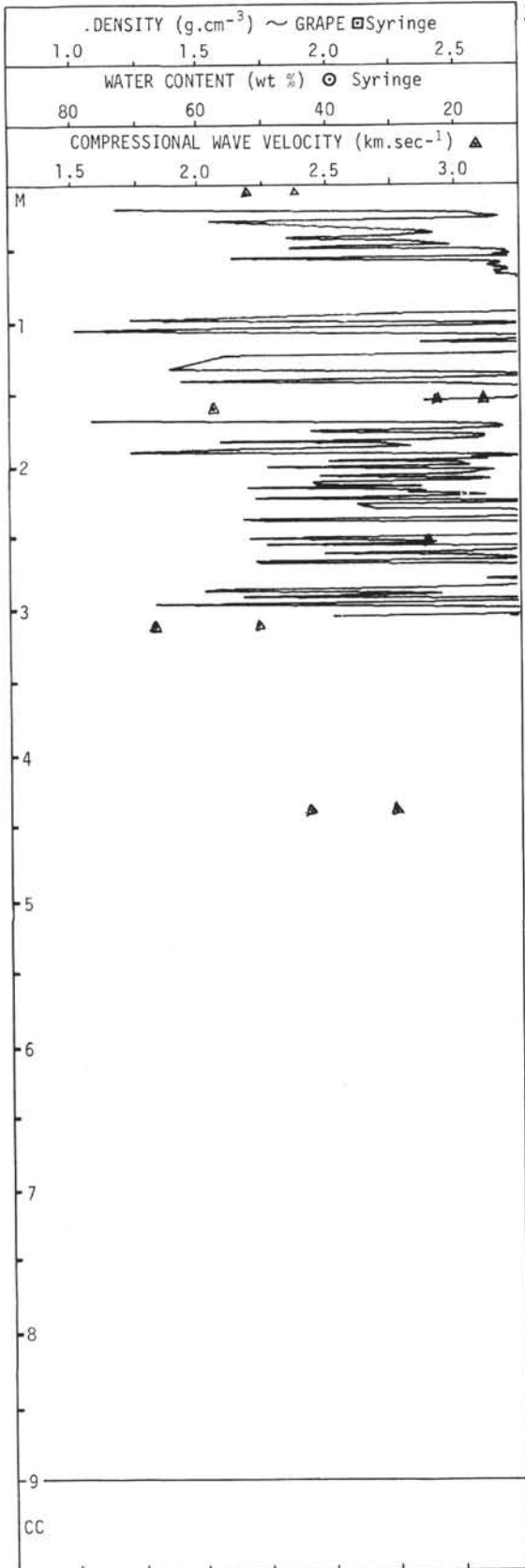


337-13



For Explanatory Notes, see Chapter 1

337-14



For Explanatory Notes, see Chapter 1

